port from University of Guanajuato. Mendoza-Macias C.L. received a doctoral fellowship from CONACYT (Mexico).

References

Ago, H., Oda, M., Takahashi, M., Tsuge, H., Ochi, S., Katunuma, N., Miyano, M., Sakurai, J., 2006. Structural basis of the sphingomyelin phosphodiesterase activity in neutral sphingomyelinase from *Bacillus cereus*. The Journal of Biological Chemistry 281, 16157–16167.

Alley, S.B., Scott, W.A., Cohn, Z.A., 1980. Plasma membrane of *Entamoeba histolytica*. The Journal of Experimental Medicine 152, 391–404.

Bramley, A.J., Patel, A.H., O'Reilly, M., Foster, R., Foster, T.J., 1989. Roles of alpha-toxin and beta-toxin in virulence of *Staphylococcus aureus* for the mouse mammary gland. Infection and Immunity 57, 2489–2494.

Castillo, S.S., Levy, M., Thaikoottathil, J.V., Goldkorn, T., 2007. Reactive nitrogen and oxygen species activate different sphingomyelinase to induce apoptosis in airway epithelial cells. Experimental Cell Research 313, 2680–2686.

Cerbón, J., Olguin, T., Alvarez-Grave, P.R., López-Sánchez, R.C., 2009. *Entamoeba invadens*: sphingolipids metabolic regulation is the main component of a PKC signaling pathway in controlling cell growth and proliferation. Experimental Parasitology 122, 106–111.

Clarke, C.J., Hannun, Y.A., 2006. Neutral sphingomyelinases and nSMase2: bridging the gaps. Biochimica et Biophysica Acta 1758, 1893–1901.

Corcoran, C.A., He, Q., Ponnusamy, S., Ogretmen, B., Huang, Y., Sheikh, M.S., 2008. Neutral sphingomyelinase-3 is a DNA damage and nongenotoxic stress-regulated gene that is deregulated in human malignancies. Molecular Cancer Research 6, 795–807.

Diamond, L.S., Harlow, D.R., Cunnick, C.C., 1978. A new medium for the axenic cultivation of *Entamoeba histolytica* and other *Entamoeba*. Transactions of the Royal Society of Tropical Medicine and Hygiene 72, 431–432.

Goñi, F.M., Alonso, A., 2002. Sphingomyelinases: enzymology and membrane activity. FEBS Letters 531, 38–46.

González-Zorn, B., Domínguez-Bernal, G., Suárez, M., Ripio, M.T., Vega, Y., Novella, S., Vázquez-Boland, J.A., 1999. The smcL gene of *Listeria ivanovii* encodes a sphingomyelinase C that mediates bacterial escape from the phagocytic vacuole. Molecular Microbiology 33, 510–523.

Grassme, H., Jekle, A., Riehle, A., Schwarz, H., Berger, J., Sandhoff, K., Kolesnick, R., Gulbins, E., 2001. CD95 signaling via ceramide-rich membrane rafts. The Journal of Biological Chemistry 276, 20589–20596.

Hanada, K., Mitamura, T., Fukasawa, M., Magistrado, P.A., Horii, T., Nishijima, M., 2000. Neutral sphingomyelinase activity dependent on Mg^{2+} and anionic phospholipids in the intraerythrocytic malaria parasite *Plasmodium falciparum*. The Biochemical Journal 346, 671–677.

Hanada, K., Palacpac, N.M., Magistrado, P.A., Kurokawa, K., Rai, G., Sakata, D., Hara, T., Horii, T., Nishijima, M., Mitamura, T., 2002. *Plasmodium falciparum* phospholipase C hydrolyzing sphingomyelin and lysocholinephospholipids is a possible target for malaria chemotherapy. The Journal of Experimental Medicine 195, 23–34.

Haque, R., Duggal, P., Ali, I.M., Hossain, M.B., Mondal, D., Sack, R.B., Farr, B.M., Beaty, T.H., Petri Jr., W.A., 2002. Innate and acquired resistance to amebiasis in Bangladesh children. The Journal of Infectious Diseases 186, 547–552.

Hernandez, Y., Shpak, M., Duarte, T.T., Mendez, T.L., Maldonado, R.A., Roychowdhury, S., Rodrigues, M.L., Das, S., 2008. Novel role of sphingolipid synthesis genes in regulating giardial encystation. Infection and Immunity 76, 2939–2949.

Krönke, M., 1999. Involvement of sphingomyelinases in TNF signaling pathways. Chemistry and Physics of Lipids 102, 157–166.

Krut, O., Wiegmann, K., Kashkar, H., Yazdanpanah, B., Krönke, M., 2006. Novel tumor necrosis factor-responsive mammalian neutral sphingomyelinase-3 is a C-tail-anchored protein. The Journal of Biological Chemistry 281, 13784–13793.

Larsson, A., Sjoquist, J., 1988. Chicken antibodies: a tool to avoid false positive results by rheumatoid factor in latex fixation tests. Journal of Immunological Methods 108, 205–208.

Laughlin, R.C., McGugan, G.C., Powell, R.R., Welter, B.H., Temesvari, L.A., 2004. Involvement of raft-like plasma membrane domains of *Entamoeba histolytica* in pinocytosis and adhesion. Infection and Immunity 72, 5349–5357.

Levade, T., Jaffrézou, J.P., 1999. Signalling sphingomyelinases: which, where, how and why? Biochimica et Biophysica Acta 1438, 1–17.

Liu, B., Hassler, D.F., Smith, G.K., Weaver, K., Hannun, Y.A., 1998. Purification and characterization of a membrane bound neutral pH optimum magnesium-dependent and phosphatidylserine-stimulated sphingomyelinase from rat brain. The Journal of Biological Chemistry 273, 34472–34479.

Loftus, B., Anderson, I., Davies, R., Alsmark, U.C., Samuelson, J., Amedeo, P., Roncaglia, P., Berriman, M., Hirt, R.P., Mann, B.J., Nozaki, T., Suh, B., Pop, M., Duchene, M., Ackers, J., Tannich, E., Leippe, M., Hofer, M., Bruchhaus, I., Willhoeft, U., Bhattacharya, A., Chillingworth, T., Churcher, C., Hance, Z., Harris, B., Harris, D., Jagels, K., Moule, S., Mungall, K., Ormond, D., Squares, R., Whitehead, S., Quail, M.A., Rabbinowitsch, E., Norbertczak, H., Price, C., Wang, Z., Guillen, N., Gilchrist, C., Stroup, S.E., Bhattacharya, S., Lohia, A., Foster, P.G., Sicheritz-Ponten, T., Weber, C., Singh, U., Mukherjee, C., El-Sayed, N.M., Petri Jr, W.A., Clark, C.G., Embley, T.M., Barrell, B., Fraser, C.M., Hall, N., 2005. The genome of the protist parasite *Entamoeba histolytica*. Nature 433, 865–868.

Long-Krug, S.A., Fischer, K.J., Hysmith, R.M., Ravdin, J.I., 1985. Phospholipase A enzymes of *Entamoeba histolytica*: description and subcellular localization. The Journal of Infectious Diseases 152, 536–541.

López-Revilla, R., Said-Fernández, S., 1980. Cytopathogenicity of *Entamoeba histolytica*: hemolytic activity of trophozoite homogenates. The American Journal of Tropical Medicine and Hygiene 29, 209–212.

MacFarlane, R.C., Singh, U., 2006. Identification of differentially expressed genes in virulent and nonvirulent *Entamoeba* species: potential implications for amebic pathogenesis. Infection and Immunity 74, 340–351.

Marchesini, N., Hannun, Y.A., 2004. Acid and neutral sphingomyelinases: roles and mechanisms of regulation. Biochemistry and Cell Biology 82, 27–44.

Matmati, N., Hannun, Y.A., 2008. ISC1 (inositol phosphosphingolipid-phospholipase C), the yeast homologue of neutral sphingomyelinases. Journal of Lipid Research 49, 922–928.

McLaughlin, J., Meerovitch, E., 1975. The surface and cytoplasmic membranes of *Entamoeba invadens* (Rodhain 1934)-II. Polypeptide and phospholipid composition. Comparative Biochemistry and Physiology, B 52, 487–497.

Mendoza-Macías, C.L., Barrios-Ceballos, M.P., de la Peña, L.P., Rangel-Serrano, A., Anaya-Velázquez, F., Mirelman, D., Padilla-Vaca, F., 2009. *Entamoeba histolytica*: effect on virulence, growth and gene expression in response to monoxenic culture with *Escherichia coli* 055. Experimental Parasitology 121, 167–174.

Mittal, K., Welter, B.H., Temesvari, L.A., 2008. *Entamoeba histolytica*: lipid rafts are involved in adhesion of trophozoites to host extracellular matrix components. Experimental Parasitology 120, 127–134.

Nakai, K., Kanehisa, M., 1992. A knowledge base for predicting protein localization sites in eukaryotic cells. Genomics 14, 897–911.

Nara, F., Tanaka, M., Masuda-Inoue, S., Yamasato, Y., Doi-Yoshioka, H., Suzuki-Konagai, K., Kumakura, S., Ogita, T., 1999. Biological activities of scyphostatin, a neutral sphingomyelinase inhibitor from a discomycete, *Trichopeziza mollissima*. The Journal of Antibiotics (Tokyo) 52, 531–535.

Nielsen, H., Engelbrecht, J., Brunak, S., von Heijne, G., 1997. Identification of prokaryotic and eukaryotic signal peptides and prediction of their cleavage sites. Protein Engineering 10, 1–6.

Nozaki, T., Asai, T., Sanchez, L.B., Kobayashi, S., Nakazawa, M., Takeuchi, T., 1999. Characterization of the gene encoding serine acetyltransferase, a regulated enzyme of cysteine biosynthesis from the protist parasites *Entamoeba histolytica* and *Entamoeba dispar*. Regulation and possible function of the cysteine biosynthetic pathway in *Entamoeba*. The Journal of Biological Chemistry 274, 32445–32452.

Okazaki, T., Bielawska, A., Domae, N., Bell, R.M., Hannun, Y.A., 1994. Characteristics and partial purification of a novel cytosolic, magnesium-independent, neutral sphingomyelinase activated in the early signal transduction of 1a, 25-dihydroxyvitamin D3-induced HL-60 cell differentiation. The Journal of Biological Chemistry 269, 4070–4077.

Openshaw, A.E., Race, P.R., Monzó, H.J., Vázquez-Boland, J.A., Banfield, M.J., 2005. Crystal structure of SmcL, a bacterial neutral sphingomyelinase C from *Listeria*. The Journal of Biological Chemistry 280, 35011–35017.

Projan, S.J., Kornblum, J., Kreiswirth, B., Moghazeh, S.L., Eisner, W., Novick, R.P., 1989. Nucleotide sequence. the beta-hemolysin gene of *Staphylococcus aureus*. Nucleic Acids Research 17, 3305.

Said-Fernández, S., López-Revilla, R., 1988. Free fatty acids released from phospholipids are the major heat-stable hemolytic factor of *Entamoeba histolytica* trophozoites. Infection and Immunity 56, 874–879.

Saito-Nakano, Y., Yasuda, T., Nakada-Tsukui, K., Leippe, M., Nozaki, T., 2004. Rab5-associated vacuoles play a unique role in phagocytosis of the enteric protozoan parasite *Entamoeba histolytica*. The Journal of Biological Chemistry 279, 49497–49507.

Schenck, M., Carpinteiro, A., Grassmé, H., Lang, F., Gulbins, E., 2007. Ceramide: physiological and pathophysiological aspects. Archives of Biochemistry and Biophysics 462, 171–175.

Segers, R.P., van der Drift, A., de Nijs, A., Corcione, P., van der Zeijst, B.A., Gaastra, W., 1990. Molecular analysis of a sphingomyelinase C gene from *Leptospira interrogans* serovar hardjo. Infection and Immunity 58, 2177–2185.

Steinbrecher, U.P., Gómez-Muñoz, A., Duronio, V., 2004. Acid sphingomyelinase in macrophage apoptosis. Current Opinion in Lipidology 15, 531–537.

Sueyoshi, N., Kita, K., Okino, N., Sakaguchi, K., Nakamura, T., Ito, M., 2002. Molecular cloning and expression of Mn(2+)-dependent sphingomyelinase/hemolysin of an aquatic bacterium, *Pseudomonas sp.* strain TK4. Journal of Bacteriology 184, 540–546.

Thompson, J.D., Higgins, D.G., Gibson, T.J., 1994. CLUSTAL W: improving the sensitivity of progressive multiple sequence alignment through sequence weighting, position-specific gap penalties and weight matrix choice. Nucleic Acids Research 22, 4673–4680.

Villalba, J.D., Gómez, C., Medel, O., Sánchez, V., Carrero, J.C., Shibayama, M., Ishiwara, D.G., 2007. Programmed cell death in *Entamoeba histolytica* induced by the aminoglycoside G418. Microbiology 153, 3852–3863.

World Health Organization, 1997. World Health Organization/Pan American Health Organization/UNESCO report of a consultation of experts on amebiasis. WHO Weekly Epidemiologic Record 72, 97–100.

Wu, J., Nilsson, A., Jönsson, B.A., Stenstad, H., Agace, W., Cheng, Y., Duan, R.D., 2006. Intestinal alkaline sphingomyelinase hydrolyses and inactivates platelet-activating factor by a phospholipase C activity. The Biochemical Journal 394, 299–308.

Yamada, A., Tsukagoshi, N., Udaka, S., Sasaki, T., Makino, S., Nakamura, S., Little, C., Tomita, M., Ikezawa, H., 1988. Nucleotide sequence and expression in *Escherichia coli* of the gene coding for sphingomyelinase of *Bacillus cereus*. European Journal of Biochemistry 175, 213–220.

Zhang, Y., Li, X., Carpinteiro, A., Gulbins, E., 2008. Acid sphingomyelinase amplifies redox signaling in *Pseudomonas aeruginosa*-induced macrophage apoptosis. Journal of Immunology 181, 4247–4254.

Mishra et al. BMC Research Notes 2010, 3:52
http://www.biomedcentral.com/1756-0500/3/52

BMC Research Notes

SHORT REPORT Open Access

Entamoeba histolytica Phosphoserine aminotransferase (EhPSAT): insights into the structure-function relationship

Vibhor Mishra[1], Vahab Ali[2], Tomoyoshi Nozaki[3], Vinod Bhakuni[1*]

Abstract

Background: Presence of phosphorylated Serine biosynthesis pathway upstream to the de novo cysteine biosynthesis pathway makes PSAT a crucial enzyme. Besides this, phoshoserine produced by the enzyme can also be taken up directly by cysteine synthase as a substrate. PSAT is a PLP dependent enzyme where the cofactor serves as an epicenter for functional catalysis with the active site architecture playing crucial role in optimum function of the enzyme.

Findings: EhPSAT is a homodimer of molecular mass 86 kDa. To understand the structural modulations associated with pH dependent changes in functional activity of EhPSAT detailed biophysical studies were carried out. pH alterations had no significant effect on the secondary structure, cofactor orientation and oligomeric configuration of the enzyme however, pH dependent compaction in molecular dimensions was observed. Most interestingly, a direct correlation between pH induced modulation of functional activity and orientation of Trp 101 present in the active site of the enzyme was observed. Sodium halides nullified the pH induced global changes in the enzyme, however differential effect of these salts on the active site microenvironment and functional activity of the enzyme was observed.

Conclusions: The study unequivocally demonstrates that pH induced selective modification of active site microenvironment and not global change in structure or oligomeric status of the enzyme is responsible for the pH dependent change in enzymatic activity of PSAT.

Background

PSAT is a vitamin B_6-dependent enzyme that belongs to the α-family of pyridoxal-5'-phosphate (PLP) enzymes. It catalyzes the reversible conversion of 3-phosphohydroxypyruvate to L-phosphoserine in a glutamate linked transamination reaction, the second step of phosphorylated serine biosynthetic pathway. Earlier studies on PSAT from *E coli* [1], *Bacillus alcalophilus* [2], *Arabidopsis thaliana* [3], and *Homo sapiens* [4] suggests that the enzyme exist as a homodimer with a subunit molecular mass between 40 to 48 kDa. Each subunit is predominantly composed of two domains, a large PLP binding domain and a small domain comprising of C-terminal part along with a short N-terminal portion [1]. Structurally PSAT is a α/β protein with one PLP molecule present in the active site, per monomer. The dimeric configuration of the enzyme is essential for the functional activity [5]. The active site amino acid residues are nearly conserved in all PSATs (Fig. 1A).

Entamoeba histolytica is a protozoan parasite that infects the gastrointestinal tract and causes amoebic colitis and extra intestinal abscesses in humans [6]. Role of L- serine in a number of important metabolic pathways in the parasite has been well established [7,8] Predominantly it serves as a precursor molecule for L-cysteine biosynthesis which plays important role in survival, growth, attachment [9,10], anti-oxidative defense [11], and Fe-S cluster biosynthesis [12]. From the amino acid sequence alignment and phylogenetic analyses EhPSAT shows close association with bacteroide PSAT [13].

* Correspondence: bhakuniv@rediffmail.com
[1]Division of Molecular and Structural Biology, Central Drug Research Institute, Chattar Manzil Palace, Council of scientific and industrial research (CSIR), Lucknow 226001, India

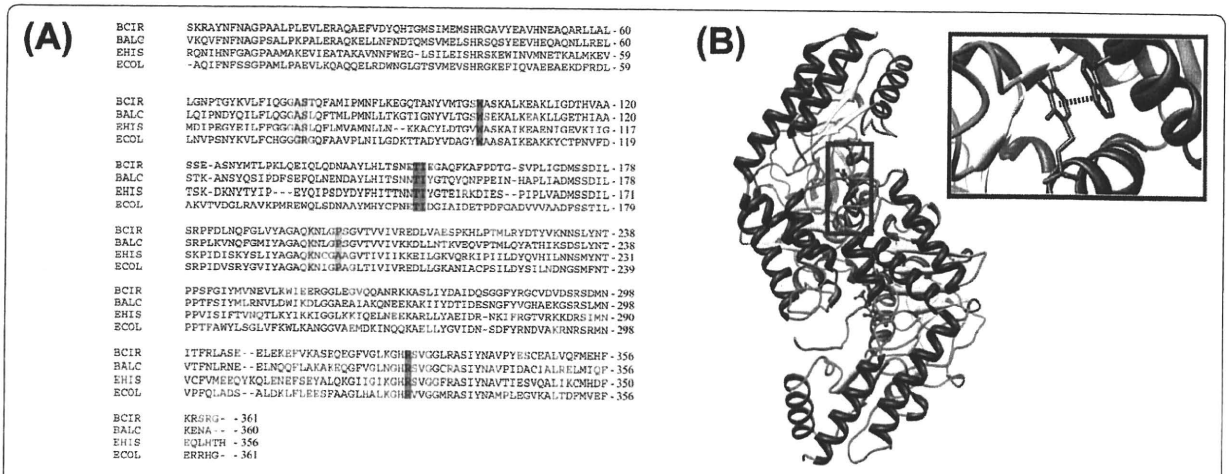

Figure 1 (A) Alignment of the amino acid sequence of PSAT from *Bacillus circulans* spp. *Alkalophilus* (BCIR), *Bacillus alcalophilus* (BALC), *Entamoeba histolytica* (EHIS), and *E coli* (ECOL). Highlighted letters indicate active site residues that interact with the cofactor PLP (light grey) and Cl^- ions (dark grey). The substitution of Pro201 (BCIR PSAT) to Ala195 (EhPSAT) in the loop region has been highlighted in blue. (B) Homology model of EhPSAT dimer visualized through UCSF chimera. The cofactor PLP present in the active site is represented in cyan color. The inset shows stacking of the cofactor PLP(cyan color) and the Trp101(brown color) at the active site.

The cofactor PLP plays a significant role in structural stabilization of PSAT from extremophiles [14] and serves as a vital tool for understanding the active site stochiometry and conformational rearrangements under various experimental conditions. We have carried out a detailed study on the pH induced changes in the functional, structural and stability properties of EhPSAT and effect of salts on these changes. Additional file 1 carries detailed information regarding the materials and experimental procedures applied in the presented study.

Results

EhPSAT production and oligomeric state

The purified protein was homogenous as indicated by a single protein band on SDS-PAGE (Fig. 2A) and a single peak in ESI-MS of molecular mass about 43 kDa (data not shown). The SEC profile of EhPSAT (Fig. 3A) along with glutaraldehyde crosslinking experiments (Fig. 3B) demonstrates that the recombinant EhPSAT is a homodimer under physiological conditions.

pH dependent changes in functional and structural properties of EhPSAT

Functional property

EhPSAT showed pH dependent bell shaped enzymatic activity profile for forward reaction with maximum activity at pH 8.5 (Fig. 2B). At pH 10 and 6.0, the enzyme retained about 50% and 20% residual activity, respectively.

For understanding the structural basis of such a characteristic pH dependence of enzymatic activity, structural changes in the enzyme under these conditions, were studied.

Secondary structure

The secondary structure elements are generally conserved among PSAT family of enzymes [1,2]. The secondary structure of EhPSAT as characterized by far-UV CD shows that it is a α/β type protein (Fig. 2C inset). No significant alterations in the CD signal at 222 nm were observed for the enzyme between pH 9 and 6(Fig. 2C). Hence, pH change does not significantly affect the secondary structure of EhPSAT.

Active site microenvironment

No significant alteration in fluorescence polarization of PLP was observed between pH 6 to 9 suggesting no change in orientation of cofactor PLP of EhPSAT with change in pH (Fig. 2D). Interestingly for tryptophan residues, with decrease in pH from 10 to 6 an almost linear enhancement in fluorescence polarization was observed, (Fig. 2E). This demonstrates that low pH induces restriction in orientation of tryptophan moiety present in enzyme. EhPSAT contains 3 tryptophan residues, two in the N-terminal region and one, Trp 101, in the active site. We wanted to see whether the above observed changes correspond to the active site tryptophan moiety or not.

On reduction of PLP aldimine, the cofactor serves as a reporter molecule itself and also as an energy acceptor of tryptophan fluorescence provided the two moieties are within a distance of 5 Å [15,16]. For EhPSAT, PLP and Trp 101 are stacked close to each other at the active site (Fig. 1B inset). Fig. 2F summarizes the effect of pH on the fluorescence spectra of EhPSAT on excitation at 295 nm. At pH 8.0 and 9.0, single fluorescence emission maxima at 335 nm and 340 nm, respectively

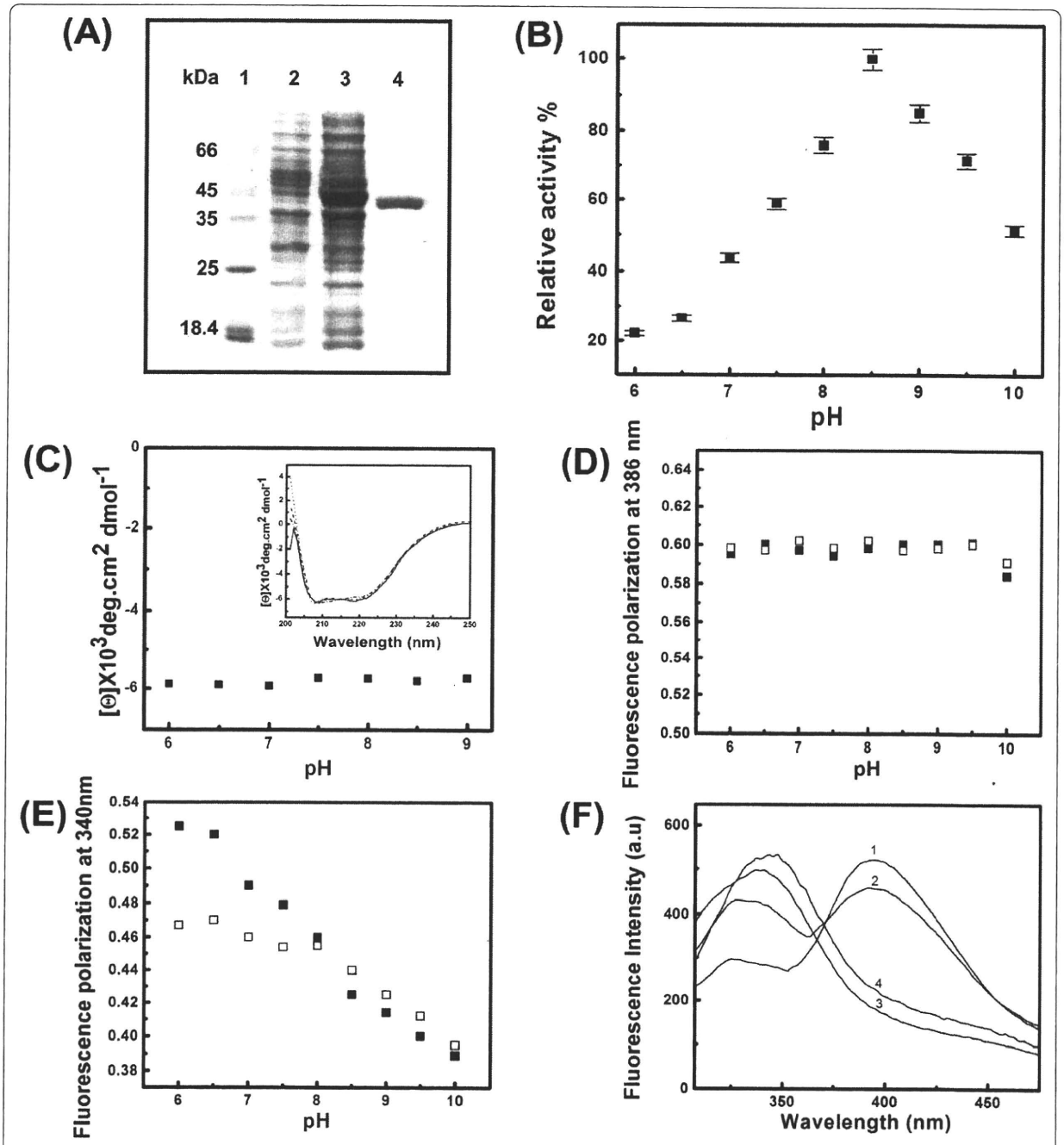

Figure 2 Overexpression, purification, functional activity and pH dependent structural changes of EhPSAT. (A) SDS-PAGE analysis of *E coli* lysate over expressing EhPSAT and the purified protein. Lanes 1-4 represent molecular weight markers, uninduced culture, induced culture and purified protein, respectively. (B) pH-dependent enzymatic activity profile of EhPSAT. The data has been represented as percentage relative activity with highest activity observed at pH 8.5 taken as 100%, each point representing mean ± SD of three independent measurements. (C) pH induced changes in the secondary structure of EhPSAT. The effect of pH on the CD signal at 222 nm. The inset shows far-UV CD spectra at pH 6 (solid line), 7 (dashed line), 8 (dotted line) and 9 (dash-dotted line), respectively. (D) and (E) pH-induced changes in PyP and Trp fluorescence polarization, respectively. In both the panels the filled and the open symbols represent protein samples in absence and presence of 200 mM NaCl, respectively. (F) pH induced changes in fluorescence emission spectra of EhPSAT excited at 295 nm. The curves 1-4 represent protein samples incubated at pH 6, 7, 8 and 9, respectively.

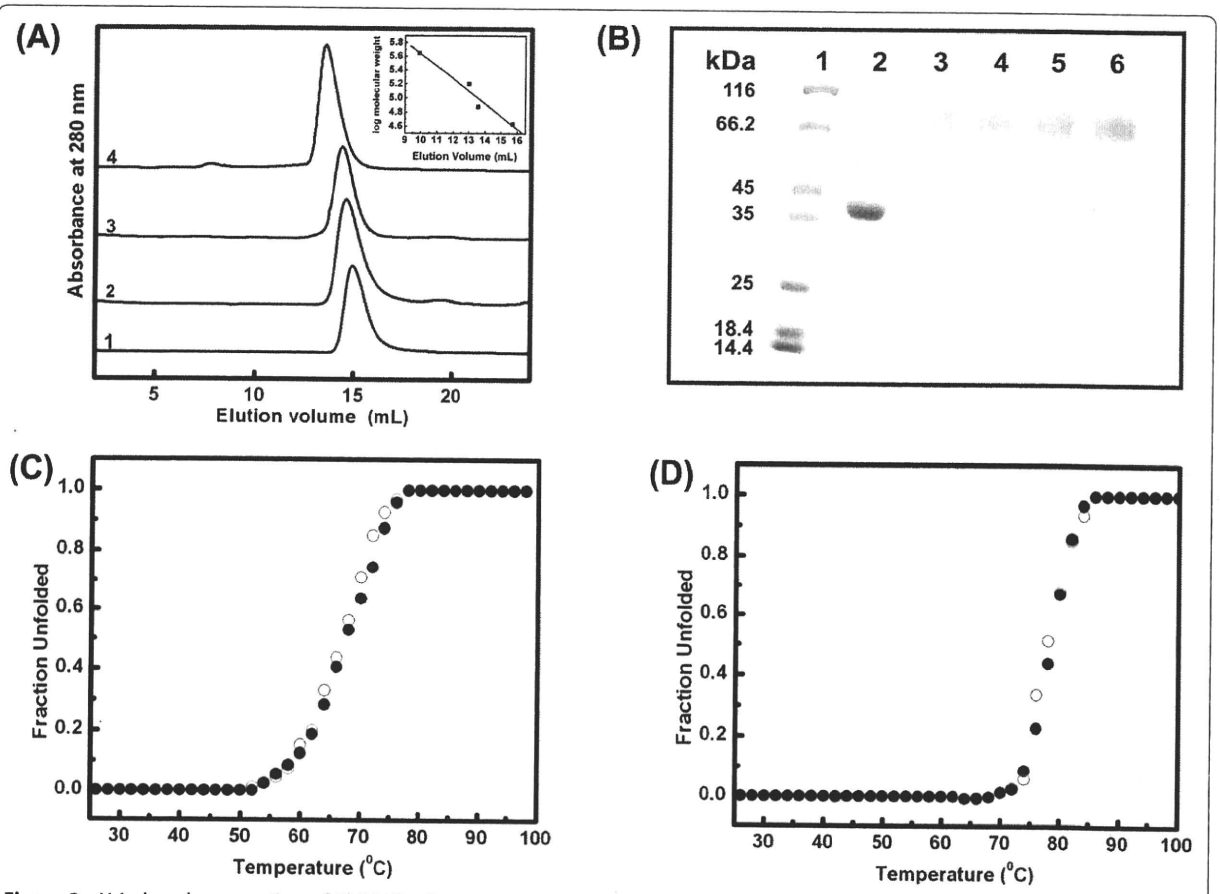

Figure 3 pH induced compaction of EhPSAT, oligomeric state and thermal stability. (A) Curves 1-4 represent SEC profile of EhPSAT on a superdex 200, 10/300 GL column at pH 6, 7, 8 and 9, respectively. The inset shows the graph of elution volume plotted against standard molecular mass markers. The proteins are (1) 440 KDa (ferritin), (2)158 KDa (aldolase), (3) 75 KDa (conalbumin) and (4) 43 KDa (ovalbumin). (B) 10% SDS-PAGE profile of glutaraldehyde crosslinked sample of EhPSAT incubated at different pH. Lane 1-6 represent molecular weight markers, uncrosslinked EhPSAT, and glutaraldehyde crosslinked form of EhPSAT at pH 9, 8, 7 and 6, respectively. Cooperative thermal unfolding of EhPSAT at pH 8.5 (panel C) and 6 (panel D) as measured by loss of CD ellepticity at 222 nm and 415 nm. A linear extrapolation of baselines in pre and post transition regions was used to determine the fraction unfolded protein within the transition region by assuming a two state mechanism of unfolding. The open and filled circle represent for far and near UV-CD signals, respectively. The thermal transition of the enzyme was found to be irreversible with precipitation observed at the end of the scan.

was observed. However, at pH 6 and 7, two clear emission maxima centered at 386 and 335 nm, respectively were observed. Furthermore, on decrease in pH from 9 to 6, a decrease in intensity of signal at 335 nm and a concomitant increase in intensity of signal at 386 nm were observed. These observations demonstrate that between pH 9 and 6 the two fluorophores PLP and Trp101 come closer to each other and show FRET. The FRET studies along with the PLP polarization studies (Fig. 2D to 2F) demonstrate that with change in pH, the orientation of Trp101 residue is modified such that it comes close to PLP cofactor in 3D space.

Molecular dimension, Subunit configuration and stability

On decrease in pH from 9 to 6, decrease in the hydrodynamic radii of the enzyme (Fig. 3A) was observed indicating either pH-induced dissociation of native dimer to monomer or compaction of dimeric conformation. Chemical crosslinking is a well accepted technique for studying changes in the oligomeric status of a protein under experimental conditions [16-21]. Fig. 3B shows the SDS PAGE profile of the glutaraldehyde cross linked protein samples. A single species corresponding to dimer of enzyme was observed under all the conditions studied. The stability of dimeric configuration over a broad pH range has also been reported for PSAT from *Bacillus circulans* ssp. *Alkalophilus*. These studies collectively demonstrate that PSAT dimer is stable over a broad pH range.

Fig. 3C and 3D shows thermal denaturation profile of EhPSAT at pH 8.5 and 6 as monitored by the loss of CD signal at 222 and 415 nm. Superimposable far-UV

and near UV CD signals demonstrate a high degree of structural cooperativity exist in EhPSAT under these conditions. However, for pH 8.5 and 6, T_m of about 67° C and 79°C, respectively were observed. These obeservations are in agreement with the ProTherm database as reported earlier for *Bacillus circulans* ssp. *Alkalophilus* [14]. Hence, decrease in pH leads to enhanced thermal stability of PSAT.

Effect of sodium halides on the enzymatic activity

Salts affect the physico-chemical properties of proteins primarily through modulation of electrostatic and hydrophobic interactions acting on the protein molecule. Fig. 4A shows the effect of 200 mM NaF, NaCl and NaBr on the enzymatic activity at pH 8.5. NaCl and NaBr inhibited the enzymatic activity in a concentration dependent manner, while NaF showed no such effect. Detailed studies with NaCl and NaF on pH induced changes in the functional activity (Fig. 4B) clearly show no significant change in the pH dependence of enzymatic activity for NaF. Interestingly, in presence of NaCl the maximum activity was found to be retained over a broader range of pH 7.5 to 8.5 and even at pH 6 about 40% residual activity was observed.

Effect of NaCl and NaF on pH induced modification at the active site and strain of internal aldimine of EhPSAT

With change in pH from 8.5 to 6 in the presence of NaCl, no effect on fluorescence polarization of PLP was observed (Fig. 2D). However, the tryptophan fluorescence polarization was found to enhance under these conditions, but to a significantly lower extent as compared to that in absence of NaCl. This demonstrates that the pH-induced change in orientation of tryptophan residue is modulated by the presence of NaCl (Fig. 2E). FRET analyses also support these observations, Fig. 4C and 4D show no significant alteration in the tryptophan microenvironment in presence of NaCl between pH 9 and 6. In contrast for NaF, FRET profile similar to that in absence of salt was observed (Fig. 2F).

The first step in the catalytic mechanism of the enzyme is transfer of a proton of charged substrate amino group to the unprotonated imine nitrogen of the internal Shiff's base in the Michaelis complex. This is followed by nucleophilic attack of the substrate amino group on C4' carbon atom of the cofactor resulting in formation of external aldimine intermediate between PLP and substrate. In PLP catalysis, the electron sink property of cofactor plays an important role. It has been proposed that in the catalytic mechanism the strain and distortion of conjugated π-electron system of PLP and internal aldimine in PSAT are important [22]. When the internal aldimine is protonated a single positive CD band is observed at 410-415 nm but it is shifted to 345-350 nm when the internal aldimine is deprotonated [22]. The additional file 2 shows the pH dependence of

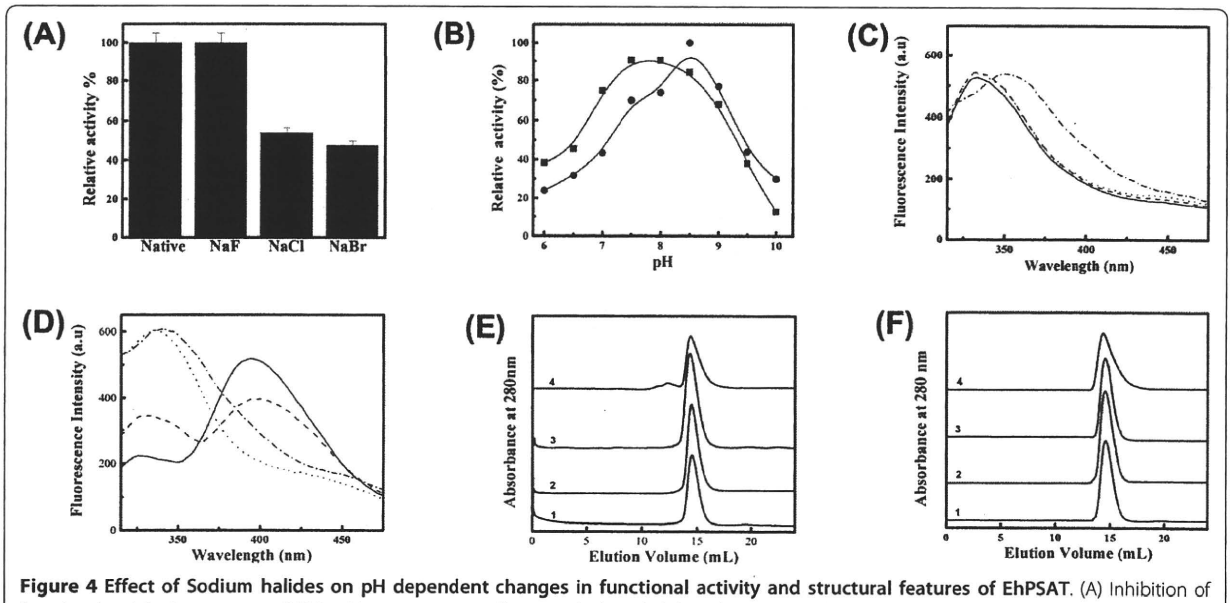

Figure 4 Effect of Sodium halides on pH dependent changes in functional activity and structural features of EhPSAT. (A) Inhibition of functional activity in presence of 200 mM concentration of various Sodium halides. The activity of EhPSAT in absence of salt (native protein) at pH 8.5 was taken as 100%. (B) pH dependent enzymatic activity profile of EhPSAT in presence of 200 mM concentration of NaCl (rectangles) and NaF (circles), respectively. For samples in presence of NaCl and NaF the highest value observed was taken as 100%. Fluorescence emission spectra of EhPSAT in presence of 200 mM NaCl (Panel C) and NaF (Panel D) at different pH. The different curves in both the panel represent protein samples at pH 6 (solid line), 7 (dashed line), 8 (dotted line) and 9 (dash dotted line). SEC profile at various pH in presence of NaCl (panel E) and NaF (panel F). The curves 1-4 represent SEC profile in presence of 200 mM concentration of salts at pH 6, 7 and 8, and 9 respectively.

near-UV CD spectra of EhPSAT in presence and absence of NaCl. Under both conditions, between pH 6 and 8, a major CD band at 410-415 nm was observed suggesting that the protein is predominantly in protonated state under these conditions. However, for protein samples at pH 9 and 10 the major CD band is shifted to 345-350 nm suggesting that the protein is predominantly in unprotonated state. These observations indicate that the pH- induced difference in the functional activity in absence and presence of NaCl is not due to modulation of pKa of the catalytic reaction.

Effect of NaCl and NAF on pH-induced compaction and thermal unfolding of EhPSAT

Fig. 4E and 4F, presents the SEC profile of EhPSAT at pH 6,7,8 and 9 in presence of 200 mM NaCl and NaF, respectively. No significant change in molecular dimension of the protein with change in pH was observed suggesting that pH induced compaction is abolished by salts. Fig. 5A to 5D, shows the thermal unfolding at pH 8.5 and 6.0, respectively in presence of 200 mM NaCl and NaF. At pH 8.5, a significant difference in *Tm* associated with loss of secondary structure and dissociation of PLP from enzyme was observed suggesting the thermal denaturation process in presence of salts to be a noncooperative event. However, at pH 6.0 in presence of salts changes similar to that in absence of salts were observed.

Discussion

The active site of PSAT is optimized for binding of L-glutamate, 3-phosphohydroxy pyruvate, 2-oxoglutarate and L-phosphoserine [1]. Structural fluctuations in the native state of protein significantly influence the functional activity [23]. The secondary structure of EhPSAT is resistant to pH change between 9 and 6 similar to

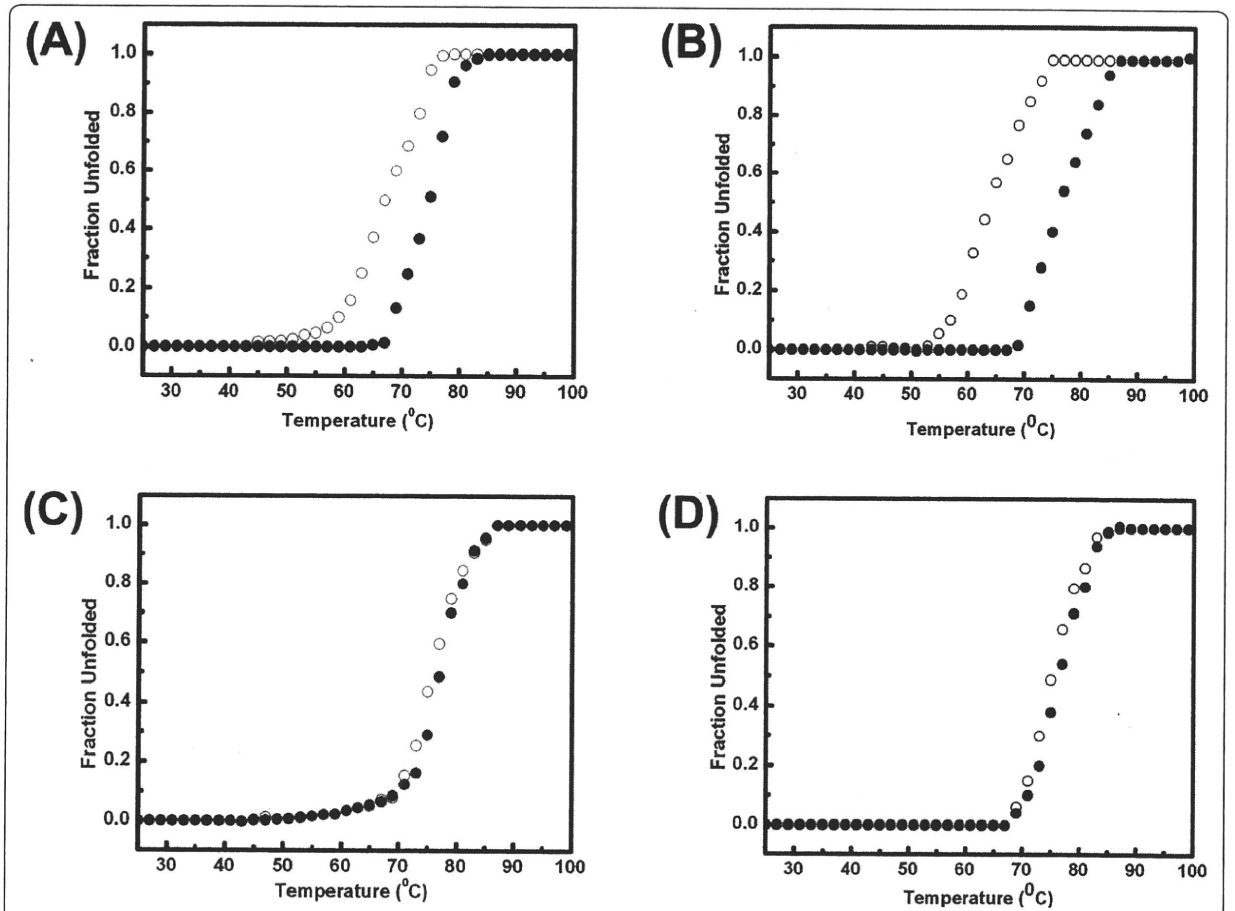

Figure 5 Thermal unfolding in presence of Sodium halides. Thermal denaturation profile at pH 8.5 in presence of 200 mM NaCl (panel A), NaF (panel B) and at pH 6 in presence of 200 mM NaCl (panel C) and NaF (panel D), respectively. The open and closed circles represent CD ellepticity measured at 222 nm and 415 nm, respectively. A linear extrapolation of baselines in pre and post transition regions was used to determine the fraction unfolded protein within the transition region by assuming a two state mechanism of unfolding. The thermal transition of the enzyme was found to be irreversible with precipitation observed at the end of the scan.

Bacillus circulans spp. *Alkalophilus* (BCIR) PSAT [14]. Hence, the secondary structure of PSATs is stable over a wide pH range and so does not play any significant role in modulation of enzymatic activity.

Crystallographic studies on BALC PSAT clearly suggest the presence of ion binding sites on PSAT molecule[2]. Four Cl^- ions in particular are found to be present 2 per monomer close to the active site residue Trp102. Main chain amides of Ser101, Trp102, Thr152 and Ile153 form the binding site for one Cl^- ion and the second one is located between positively charged side chain of Arg334 and the $N^{\varepsilon 1}$ atom of Trp102(amino acid position described according to BALC PSAT) [2]. Amino acids responsible for chloride ion binding are conserved in BALC PSAT and EhPSAT (Fig. 1A). It is possible that direct binding of Cl^- and Br^- ions (ionic radii 1.67Å and 1.96 Å, respectively) in the active site leads to structural modifications which results in significant loss of functional activity. F^- Ions being smaller in size (ionic radii 1.36 Å) will not bind to the anion binding site(s) with similar affinity and hence not bring about similar change in active site conformation as chloride or bromide ions. This possibility is also supported by the observation that SO_4^{2-} ions as they also inhibit the enzymatic activity similar to chloride or bromide ions (Data not shown).

The two active sites of PSAT dimer are situated approximately 20 Å apart at the subunit interface. In each active site a PLP molecule is bound with an aldimine linkage to Lys 191 and aditionally hydrogen bonded to residues from the two large domains, besides this prominent stacking interaction at the active site between the pyridine ring of PLP and the indole ring of Trp101, which are usually separated by a distance of approximately 5 Å, occurs on the re-face of the cofactor [[14], this study]. No change in orientation of PLP and tryptophan aromatic ring occurs upon pH change [14]. In case of EhPSAT we observed a pH dependent change in orientation of tryptophan moiety but not for the PLP as monitored by fluorescence polarization (Fig. 2D and 2E). Presence of two fluorophores predominantly stacked with each other in the active site invariably serves as an important tool for probing fine fluctuations of the pH sensitive active site microenvironment. On moving towards low pH (from 8 to 6), the enzyme starts to gradually loose its activity and under these conditions there is a gradual appearance of FRET, suggesting an inwards movement of tryptophan moiety thus bringing it close to PLP in space. In contrast, on moving towards basic pH *i.e.* from 8 towards 10, a shift of tryptophan fluorescence emission maximum from 335 nm to 340 nm was observed, which shows an opening of native conformation of enzyme with partial solvent exposure of tryptophan residue(s). Such pH dependent changes in the active site dynamics suggest relaxation (open) and compaction (close) of active site conformation. Such a dynamic movement in the active site would interfere with proper docking of substrates and responsible for loss of enzymatic activity. Support to such a possibility comes from the pH studies in presence of NaCl where no relative movement of the two fluorophores with pH change (as discussed in paper) was observed and under these conditions no significant alteration in the enzymatic activity was observed over a wider pH range. Conformational changes observed in the present study have not been reported earlier based on the comparison of crystal structures of PSAT at pH 4.6 and pH 8.5[14] because of the fact that protein crystal packing may interfere with fine conformational changes observed in the solution [24,25]. These differences in the active site microenvironment between EhPSAT and BCIR PSAT might probably be due to change in flexibility of the loop region 199-202 which is located near the active site. In this loop the Pro201 in BCIR PSAT is changed to Ala195 in EhPSAT (shown in Fig. 1). Such a change will definitely bring about differences in the flexibility of the loop and subsequently modulate the packing of the protein in the vicinity of active site. The studies presented in the paper clearly demonstrate that local changes at active site microenvironment and not global changes in the protein conformation are responsible for the pH induced modulation of functional activity of PSAT.

Additional file 1: Materials and methods. This file contains information regarding the chemicals, instrumentation and experimental procedures used in the study. This file also describes the methodology implied behind the experimental setup. This file can be opened using Microsoft word.
Click here for file
[http://www.biomedcentral.com/content/supplementary/1756-0500-3-52-S1.DOC]

Additional file 2: Near UV-CD spectra of EhPSAT. This file contains a figure showing near UV-CD spectra of EhPSAT in absence (Panel A) and presence (Panel B) of 200 mM NaCl. In both the panels the curves 1-4 represent protein samples incubated at pH 6, 7, 8 and 9 respectively. This file can be opened using adobe acrobat reader.
Click here for file
[http://www.biomedcentral.com/content/supplementary/1756-0500-3-52-S2.PDF]

Abbreviations

PSAT: phosphoserine aminotransferase; PLP: pyridoxal-5'-phosphate; Ni-NTA: nickel nitrilotriacetic acid; HPAP: hydroxypyruvic acid phosphate(also called phosphohydroxy pyruvate); SEC: size exclusion chromatography; FRET: fluorescence resonance energy transfer; ESI-MS: electrospray ionization mass spectroscopy.

Acknowledgements

VM wishes to thank Council of scientific and industrial research (CSIR), New Delhi, for financial assistance. Ashutosh kumar is acknowledged for bioinformatics analysis. Funding for article processing charges: Annual S S

Bhatnagar award fund (to VB). This is communication no.7649 from CDRI, Lucknow (India).

Author details
[1]Division of Molecular and Structural Biology, Central Drug Research Institute, Chattar Manzil Palace, Council of scientific and industrial research (CSIR), Lucknow 226001, India. [2]Department of Biochemistry, Rajendra Memorial Research Institute of Medical Sciences, AgamKuan, Patna 800007, India. [3]Department of Parasitology, National Institute of Infectious diseases, 1-23-1 Toyama, Shinjuku-Ku, Tokyo 162-8640, Japan.

Authors' contributions
VM carried out all the experiments and data analysis. VB concieved and directed the study and was responsible for final evaluation of results. VM and VB drafted the manuscript. VA and TN provided the clone of PSAT and were part of the discussions during drafting of the manuscript. All authors read and approved the final manuscript.

Competing interests
The authors declare that they have no competing interests.

Received: 3 August 2009 Accepted: 3 March 2010
Published: 3 March 2010

References

1. Hester G, Stark W, Moser M, Kallen J, Markovic-Housley Z, Jansonius JN: **Crystal structure of phosphoserine aminotransferase from Escherichia coli at 2.3 A resolution: comparison of the unligated enzyme and a complex with alpha-methyl-l-glutamate.** *J Mol Biol* 1999, **286(3)**:829-850.
2. Dubnovitsky AP, Kapetaniou EG, Papageorgiou AC: **Enzyme adaptation to alkaline pH: atomic resolution (1.08 A) structure of phosphoserine aminotransferase from Bacillus alcalophilus.** *Protein Sci* 2005, **14**:97-110.
3. Ho CL, Noji M, Saito M, Yamazaki M, Saito K: **Molecular characterization of plastidic phosphoserine aminotransferase in serine biosynthesis from Arabidopsis.** *Plant J* 1998, **16**:443-52.
4. Baek JY, Jun DY, Taub D, Kim YH: **Characterization of human phosphoserine aminotransferase involved in the phosphorylated pathway of L-serine biosynthesis.** *Biochem J* 2003, **373**:191-200.
5. John RA: **Pyridoxal phosphate-dependent enzymes.** *Biochim Biophys Acta* 1995, **1248**:81-96.
6. Ali V, Nozaki T: **Current therapeutics, their problems, and sulfur-containing-amino-acid metabolism as a novel target against infections by "amitochondriate" protozoan parasites.** *Clin Microbiol Rev* 2007, **20**:164-87.
7. Ali V, Hashimoto T, Shigeta Y, Nozaki T: **Molecular and biochemical characterization of D-phosphoglycerate dehydrogenase from Entamoeba histolytica. A unique enteric protozoan parasite that possesses both phosphorylated and nonphosphorylated serine metabolic pathways.** *Eur J Biochem* 2004, **271**:2670-81.
8. Ali V, Shigeta Y, Nozaki T: **Molecular and structural characterization of NADPH-dependent d-glycerate dehydrogenase from the enteric parasitic protist Entamoeba histolytica.** *Biochem J* 2003, **375**:729-36.
9. Gillin FD, Diamond LS: **Attachment of Entamoeba histolytica to glass in a defined maintenance medium: specific requirement for cysteine and ascorbic acid.** *J Protozool* 1980, **27**:474-8.
10. Gillin FD, Diamond LS: **Entamoeba histolytica and Giardia lamblia: growth responses to reducing agents.** *Exp Parasitol* 1981, **51**:382-91.
11. Nozaki T, Asai T, Sanchez LB, Kobayashi S, Nakazawa M, Takeuchi T: **Characterization of the gene encoding serine acetyltransferase, a regulated enzyme of cysteine biosynthesis from the protist parasites Entamoeba histolytica and Entamoeba dispar. Regulation and possible function of the cysteine biosynthetic pathway in Entamoeba.** *J Biol Chem* 1999, **274**:32445-52.
12. Ali V, Shigeta Y, Tokumoto U, Takahashi Y, Nozaki T: **An intestinal parasitic protist, Entamoeba histolytica, possesses a non-redundant nitrogen fixation-like system for iron-sulfur cluster assembly under anaerobic conditions.** *J Biol Chem* 2004, **279**:16863-74.
13. Ali V, Nozaki T: **Biochemical and functional characterization of phosphoserine aminotransferase from Entamoeba histolytica, which possesses both phosphorylated and non-phosphorylated serine metabolic pathways.** *Mol Biochem Parasitol* 2006, **145**:71-83.
14. Kapetaniou EG, Thanassoulas A, Dubnovitsky AP, Nounesis G, Papageorgiou AC: **Effect of pH on the structure and stability of Bacillus circulans ssp. alkalophilus phosphoserine aminotransferase: thermodynamic and crystallographic studies.** *Proteins* 2006, **63**:742-53.
15. Cai K, Schirch V: **Structural studies on folding intermediates of serine hydroxymethyltransferase using fluorescence resonance energy transfer.** *J Biol Chem* 1996, **271**:27311-20.
16. Chaturvedi S, Bhakuni V: **Unusual structural, functional, and stability properties of serine hydroxymethyltransferase from Mycobacterium tuberculosis.** *J Biol Chem* 2003, **278**:40793-805.
17. Mishra P, Akhtar MS, Bhakuni V: **Unusual structural features of the bacteriophage-associated hyaluronate lyase (hylp2).** *J Biol Chem* 2006, **281**:7143-50.
18. Bhatt AN, Khan MY, Bhakuni V: **The C-terminal domain of dimeric serine hydroxymethyltransferase plays a key role in stabilization of the quaternary structure and cooperative unfolding of protein: domain swapping studies with enzymes having high sequence identity.** *Protein Sci* 2004, **13**:2184-95.
19. Akhtar MS, Ahmad A, Bhakuni V: **Divalent cation induced changes in structural properties of the dimeric enzyme glucose oxidase: dual effect of dimer stabilization and dissociation with loss of cooperative interactions in enzyme monomer.** *Biochemistry* 2002, **41**:7142-9.
20. Akhtar MS, Ahmad A, Bhakuni V: **Guanidinium chloride- and urea-induced unfolding of the dimeric enzyme glucose oxidase.** *Biochemistry* 2002, **41**:3819-27.
21. Singh K, Bhakuni V: **Cation induced differential effect on structural and functional properties of Mycobacterium tuberculosis alpha-isopropylmalate synthase.** *BMC Struct Biol* 2007, **7**:39.
22. Dubnovitsky AP, Ravelli RB, Popov AN, Papageorgiou AC: **Strain relief at the active site of phosphoserine aminotransferase induced by radiation damage.** *Protein Sci* 2005, **14**:1498-507.
23. Singh K, Bhakuni V: **Toxoplasma gondii ferredoxin-NADP+ reductase: Role of ionic interactions in stabilization of native conformation and structural cooperativity.** *Proteins* 2008, **71**:1879-88.
24. Kapoor P, Sahasrabuddhe AA, Kumar A, Mitra K, Siddiqi MI, Gupta CM: **An unconventional form of actin in protozoan hemoflagellate, Leishmania.** *J Biol Chem* 2008, **283**:22760-73.
25. Rould MA, Wan Q, Joel PB, Lowey S, Trybus KM: **Crystal structures of expressed non-polymerizable monomeric actin in the ADP and ATP states.** *J Biol Chem* 2006, **281**:31909-19.

doi:10.1186/1756-0500-3-52
Cite this article as: Mishra *et al.*: *Entamoeba histolytica* Phosphoserine aminotransferase (EhPSAT): insights into the structure-function relationship. *BMC Research Notes* 2010 **3**:52.

Mukherjee *et al. Gut Pathogens* 2010, **2**:12
http://www.gutpathogens.com/content/2/1/12

Gut Pathogens

LETTER TO THE EDITOR Open Access

Trend of *Entamoeba histolytica* infestation in Kolkata

Avik K Mukherjee[1], Kaushik Das[1], Mihir K Bhattacharya[2], Tomoyoshi Nozaki[3], Sandipan Ganguly[1*]

Abstract

Background: *Entamoeba histolytica* infection is found almost all over the world and is highly endemic and a major cause of parasitic diarrhoea particularly in the developing countries.

Methods: A systemic surveillance was set up at the Infectious Disease hospital, Kolkata, India between November 2007 and October 2009 for understanding the trend of *E. histolytica* infection in Kolkata. Fecal samples were collected from diarrhoeal patients attending the hospital, under the surveillance system and processed for detection of *E. histolytica*.

Results: During the last two years about 2500 diarrhoeal samples were collected and screened for *E. histolytica*. About 3.6% were positive for *E. histolytica*. As compared to the earlier years, *E. histolytica* infection was observed to be less amongst patients screened during the last two years. No seasonality was observed in Kolkata although in the neighboring tropical country Bangladesh, a typical seasonality of *E. histolytica* infection was noticed.

Conclusion: The study indicates that the detection rate of *E. histolytica* infection amongst diarrhoeal patients in Kolkata is decreasing during the last two years than that of Bangladesh.

Background

Amoebiasis caused by infection with *E. histolytica* occurs almost all over the world and is highly endemic especially in the developing countries. It is one of the major causes of dysentery/diarrhoea in Kolkata, India. According to our previous study (unpublished), detection of *Entamoeba histolytica* showed a marked seasonality, i.e. high peak during post-monsoon and post-winter seasons. According to the reports from other tropical countries, especially in Bangladesh, which is geographically closest to Kolkata, there is a typical pattern of detection of *E. histolytic w*here *E. histolytica* usually shows its highest peaks in the wet season and gradually decreases with the arrival of dry season [1,2]. In a study in Bangladesh, it was shown that wet environment is not the only factor that affects the detection curve of *E. histolytica*, but anti-Carbohydrate Recognition Domain IgA level in the gut is another determining factor for its occurrence in a closed population [3]. However, even in that case *E. histolytica* detection followed a particular seasonality and trend. However in Kolkata the present scenario is different from other tropical regions.

Study design and results

For the last few years, we have been engaged with the surveillance study to determine the detection rate of common enteric parasites in Kolkata. During the last two years, about 2500 diarrhoeal stool samples were screened from hospitalized patients through a systematic sampling procedure as described previously [1] in collaboration with Infectious Diseases Hospital, Kolkata. In this surveillance, every fifth patient attending the Infectious diseases hospital from different parts of Kolkata with diarrhoea in randomly selected two days a week were included in the study. Fecal samples from these patients were collected and sent to the laboratory within half an hour of collection for detection of *E. histolytica* by microscopic examination using iodine wet mount method; PCR and antigen capture ELISA. The whole study was carried out from the month of November 2007 to October 2009 to include at least two seasonal cycles for better understanding of the seasonality. Although one of the major diarrhoea causing pathogen in Kolkata is *Vibrio cholerae* [4]

* Correspondence: sandipanganguly@gmail.com
[1]Department of Parasitology, National Institute of Cholera and Enteric Diseases, Indian Council of Medical Research, P33 CIT Road, Scheme XM, Kolkata - 700010, India
Full list of author information is available at the end of the article

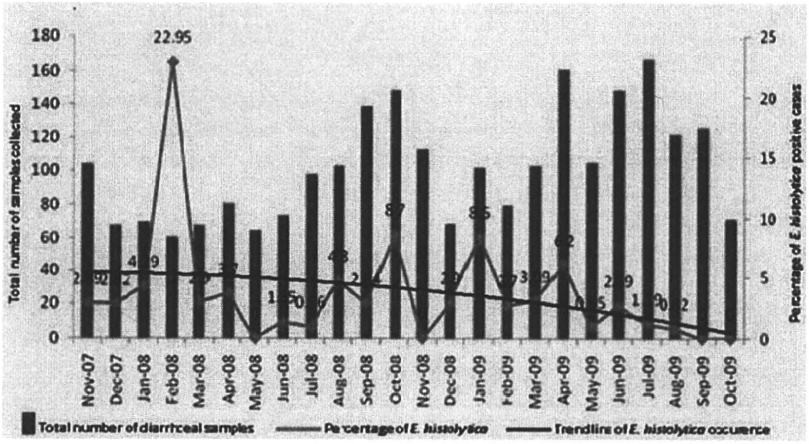

Figure 1 Month wise distribution of samples collected throughout the study period along with percentage of *E. histolytica* positive among them.

among all etiologies, *E. histolytica* (3.6%) is one of the major diarrheagenic parasites among the parasitic etiologies of diarrhoea. It caused some sporadic diarrhea throughout the study period without any particular seasonality which is uncommon for a tropical area like Kolkata. Overall a decreasing trend of *E. histolytica* infection was also seen (Figure 1). Reasons behind this different nature of infection might be due to physical and environmental factors which could influence *E. histolytica* detection rate, such as choice of common antimicrobial drug, temperature, detection procedure of *E. histolytica* etc. But none of these changed strikingly in last two years that could affect *E. histolytica* detection rate. Indiscriminate use of anti-parasitic drugs like metronidazole and tinidazole could be attributed to the decreasing trend of detection of *E. histolytica* in Kolkata.

Conclusion

The present study demonstrates that there is no particular seasonality of occurrence of *E. histolytica* infection which is not typical of a tropical area like Kolkata. A different pattern which is almost unique in comparison to other tropical countries has been observed. Contribution of environmental and host factors as well as parasite genotypes are very important for the outcome of infection [2,5]. Although no physical or environmental factor behind this changing pattern of *E. histolytica* infestation in Kolkata has yet been reported, but it is certain that *E. histolytica* is showing a slow but obvious change in its seasonality and this might be a signal for a transition period of changing nature of infestation by this parasite in this part of the world. It is worth mentioning that impact of climate change might lead to such changes, although no such studies are available.

Acknowledgements

This study was supported by grants from

1. Japan Health Science Foundation and
2. Okayama University Program of Founding Research Centre for Emerging and Reemerging Infectious Disease, Ministry of Education, Culture, Sports, Science and Technology of Japan.

Authors also acknowledge the help and support given by Prof. Y. Takeda, Dr. G. B. Nair, Dr. Samiran Panda and Dr. K. Rajendran of NICED during preparation of this letter and Debarati Ganguly of Calcutta University for her careful proof reading and correction of English in the letter.

Author details

[1]Department of Parasitology, National Institute of Cholera and Enteric Diseases, Indian Council of Medical Research, P33 CIT Road, Scheme XM, Kolkata - 700010, India. [2]Department of Clinical Medicine, National Institute of Cholera and Enteric Diseases, Indian Council of Medical Research, P33 CIT Road, Scheme XM, Kolkata - 700010, India. [3]Division of Parasitology, National Institute of Infectious Diseases, Shinjuku, Tokyo, Japan.

Received: 1 September 2010 Accepted: 6 October 2010
Published: 6 October 2010

References

1. Mukherjee AK, Chowdhury P, Bhattacharya MK, Ghosh M, Rajendran K, Ganguly S: **Hospital-based surveillance of enteric parasites in Kolkata.** *BMC Research Notes* 2009, **2**:110.
2. Ravdin JI: **Amebiasis; Series on Tropical Medicine.** *Science and Practice* Imperial College Press 2000, **2**:55.
3. Haque R, Mondal D, Duggal P, Kabir M, Roy S, Farr BM, Sack RB, Petri WA Jr: ***Entamoeba histolytica* Infection in Children and Protection from Subsequent Amebiasis.** *Infect Immunity* 2006, 904-909.
4. Nair Balakrish Gopinath, Ramamurthy Thandavarayan, Bhattacharya Kumar Mihir, Krishnan Triveni, Ganguly Sandipan, Saha Rani Dhira, Rajendran Krishnan, Manna Byomkesh, Ghosh Mrinmoy, Okamoto Keinosuke, Takeda Yoshifumi: **Emerging trends in the etiology of enteric pathogens as evidenced from an active surveillance of hospitalized diarrhoeal patients in Kolkata, India.** *Gut Pathogen* 2010, **2**:4.
5. Petri WA Jr, Mondal D, Peterson KM, Duggal P, Haque R: **Association of malnutrition with amebiasis.** *Nutr Rev* 2009, **67**:S207.

doi:10.1186/1757-4749-2-12
Cite this article as: Mukherjee *et al.*: Trend of *Entamoeba histolytica* infestation in Kolkata. *Gut Pathogens* 2010 2:12.

Experimental Parasitology 126 (2010) 337–347

Contents lists available at ScienceDirect

Experimental Parasitology

journal homepage: www.elsevier.com/locate/yexpr

Minireview

Conservation and function of Rab small GTPases in *Entamoeba*: Annotation of *E. invadens* Rab and its use for the understanding of *Entamoeba* biology

Kumiko Nakada-Tsukui, Yumiko Saito-Nakano, Afzal Husain, Tomoyoshi Nozaki *

Department of Parasitology, National Institute of Infectious Diseases, Tokyo 162-8640, Japan

ARTICLE INFO

Article history:
Received 7 November 2009
Received in revised form 19 April 2010
Accepted 19 April 2010
Available online 29 April 2010

Keywords:
Entamoeba
Rab
Small GTPase
Vesicular traffic
Encystation

ABSTRACT

Entamoeba invadens is a reptilian enteric protozoan parasite closely related to the human pathogen *Entamoeba histolytica* and a good model organism of encystation. To understand the molecular mechanism of vesicular trafficking involved in the encystation of *Entamoeba*, we examined the conservation of Rab small GTPases between the two species. *E. invadens* has over 100 Rab genes, similar to *E. histolytica*. Most of the Rab subfamilies are conserved between the two species, while a number of species-specific Rabs are also present. We annotated all *E. invadens* Rabs according to the previous nomenclature [Saito-Nakano, Y., Loftus, B.J., Hall, N., Nozaki, T., 2005. The diversity of Rab GTPases in *Entamoeba histolytica*. Experimental Parasitology 110, 244–252]. Comparative genomic analysis suggested that the fundamental vesicular traffic machinery is well conserved, while there are species-specific protein transport mechanisms. We also reviewed the function of Rabs in *Entamoeba*, and proposed the use of the annotation of *E. invadens* Rab genes to understand the ubiquitous importance of Rab-mediated membrane trafficking during important biological processes including differentiation in *Entamoeba*.

1. Introduction

Small GTP-binding proteins (GTPase) are molecular switches ubiquitously found in eukaryotes. These proteins are involved in various important cellular processes including cell proliferation, cytoskeletal assembly, and intracellular membrane traffic. Small GTPases are classified, based on their primary sequences, into five families: Ras, Rho/Rac, Rab, Sar/Arf, and Ran (Bourne et al., 1990; Takai et al., 2001). Rab small GTPases constitute the largest group of this superfamily and are essential regulators of vesicular transport (Novick and Zerial, 1997; Stenmark, 2009). Higher eukaryotes generally have a larger repertoire of Rab genes than unicellular eukaryotes. *Homo sapiens*, *Arabidopsis thaliana*, and *Drosophila melanogaster*, for example, have 60, 29, and 29 Rab genes, respectively, while *Saccharomyces cerevisiae* has only 11 (Pereira-Leal and Seabra, 2001).

Membrane traffic plays an important role in the virulence of the protozoan parasite *Entamoeba histolytica*, the causative agent of amebiasis. Regulation of membrane trafficking via Rab proteins has been well studied in *E. histolytica* (for a review, see Nozaki and Nakada-Tsukui, 2006). While a majority of parasitic protozoa possess reduced numbers of Rab genes, *E. histolytica* and *Trichomonas vaginalis* have an expanded repertoire of Rabs (Saito-Nakano et al., 2005; Carlton et al., 2007), suggesting that they rely heavily on Rab-mediated membrane trafficking. Among the more than 100 Rabs identified to date, the functions of only a half dozen *E. histolytica* Rabs, that is, EhRabA, 5, 7A, 7B, 11A, and 11B, have been demonstrated (Welter et al., 2005; Welter and Temesvari, 2009; Saito-Nakano et al., 2004; Nakada-Tsukui et al., 2005; Saito-Nakano et al., 2007; Mitra et al., 2007). Thus, the role of the complex Rab family in *Entamoba* has only started to be unveiled.

The molecular mechanisms of stage conversion between the trophozoite and cyst stages remain largely unknown in *E. histolytica* (Eichinger, 1997; Singh and Ehrenkaufer, 2009), due to the lack of an *in vitro* encystation system. Thus, encystation has been studied in *Entamoeba invadens*, a closely related reptilian pathogen that also forms quadranucleate cysts (Eichinger, 2001; Wang et al., 2003). Vesicular traffic likely plays an important role in encystation because the trophozoite degrades unnecessary components and synthesizes and transports new molecules necessary for cyst formation (Picazarri et al., 2008; Chatterjee et al., 2009). In this review, we propose the annotation of Rab genes from *E. invadens* to facilitate the understanding of the conservation and species-specific evolution of Rab in *Entamoeba*. We show that fundamental Rab-mediated vesicular trafficking is well conserved in *Entamoeba*. We also summarize and review previous studies that showed transcriptional changes of Rab genes under stress and during stage conversion in *E. histolytica*, and transcriptional differences between *E. histolytica* strains.

* Corresponding author. Address: Department of Parasitology, National Institute of Infectious Diseases, 1-23-1 Toyama, Shinjuku-ku, Tokyo 162-8640, Japan. Fax: +81 3 5285 1219x1173.
E-mail address: nozaki@nih.go.jp (T. Nozaki).

0014-4894/$ - see front matter © 2010 Elsevier Inc. All rights reserved.
doi:10.1016/j.exppara.2010.04.014

Table 1
Rab small GTPases in *E. histolytica* and *E. invadens*.

Rab subfamily	*Entamoeba histolytica*					*Entamoeba invadens*				
	EhRab isotype	Accession number	ID number	Protein length	C-terminal peptides	EiRab isotype	ID number	% Identity to Eh homologue	Protein length	C-terminal peptides
I. Rab conserved in eukaryotes										
Rab1	EhRab1A	XP_651336	EHI_108610	206	CXXX	EiRab1A	EIN_104660	83	207	CXXX
	EhRab1B	XP_649033	EHI_146510	200	XXCC	EiRab1B	EIN_033160	75	208	CXCX
Rab2	EhRab2A	XP_649924	EHI_146320	785	–	EiRab2A	EIN_200080	59	217	–
	EhRab2B	XP_649335	EHI_046390	214	–	EiRab2B	EIN_277910	84	211	–
	EhRab2C	XP_656786	EHI_067850	232	–					
Rab5	EhRab5	XP_655377	EHI_026420	196	XXCC	EiRab5A	EIN_277000	83	194	XXCC
						EiRab5B	EIN_051650	50[b]	188	XCCC
Rab21	EhRab21	XP_651927	EHI_129330	204	XXCC					
Rab7	EhRab7A	XP_649196	EHI_192810	207	XCXC	EiRab7A	EIN_112310	91	205	XXCC
	EhRab7B	XP_656820	EHI_081330	208	XCXC	EiRab7B	EIN_202680	88	206	XXCC
	EhRab7C	XP_652334	EHI_189990	198	XXCC	EiRab7C	EIN_094230	67	213	XXCC
	EhRab7D	XP_651915	EHI_082070	205	XXCC	EiRab7D	EIN_133760	80	200	XXCC
	EhRab7E	XP_651202	EHI_169280	208	XXCC	EiRab7E	EIN_148860	87	206	XXCC
	EhRab7F	XP_650338	EHI_192130	202	XXCC	EiRab7F	EIN_235870	64	206	XXCC
	EhRab7G	XP_656477	EHI_187090	191	XXCC	EiRab7G1	EIN_015310	62	197	XXCC
						EiRab7G2	EIN_299020	61	193	XXCC
	EhRab7H	XP_653414	EHI_005900	198	XXCC	EiRab7H	EIN_288760	46	203	XXCC
	EhRab7I	XP_649308	EHI_189100	205	XXCC	EiRab7I	EIN_196420	66	206	XCCX
Rab8	EhRab8A	XP_653051	EHI_199820	200	XXCC	EiRab8A	EIN_252640	48	202	XXCC
	EhRab8B	XP_652309	EHI_127380	208	XXCC	EiRab8B	EIN_149010	67	207	XXCC
Rab11	EhRab11A	XP_647948	EHI_005460	208	XXCC	EiRab11A	EIN_165880	82	208	XXCC
	EhRab11B	XP_652776	EHI_107250	212	XXCC	EiRab11B	EIN_108540	74	213	XXCC
	EhRab11C	XP_649609	EHI_161030	213	XXCC	EiRab11C	EIN_014150	71	222	XXCC
	EhRab11D	XP_652598	EHI_056100	214	XCXC	EiRab11D	EIN_050950	65	211	XXCC
II. Rab conserved in Entamoeba										
RabA	EhRabA	XP_652258	EHI_168600	199	XCXC	EiRabA	EIN_280980	85	198	XCXC
RabB	EhRabB	XP_652994	EHI_181240	193	XXCC	EiRabB	EIN_110330	69	198	XXCC
RabC	EhRabC1	XP_656355	EHI_153690	205	XXCC	EiRabC1	EIN_058650	81	198	XXCC
	EhRabC2	XP_653593	EHI_045550	207	XXCC	EiRabC2	EIN_094390	81	206	XXCC
	EhRabC3	XP_652352	EHI_143650	209	XXCC	EiRabC3A	EIN_093190	89	207	XXCC
						EiRabC3B	EIN_089560	54	213	XXCC
	EhRabC4	XP_656897	EHI_096220	204	XXCC	EiRabC4	EIN_072390	57	200	XXCC
	EhRabC5	XP_654231	EHI_122730	204	XXCC	EiRabC5	EIN_014860	73	204	XXCC
	EhRabC6	XP_654710	EHI_194280	195	XXCC					
	EhRabC7	XP_652882	EHI_079890	196	XXCC	EiRabC7	EIN_217920	70	201	XXCC
	EhRabC8	XP_651035	EHI_170390	196	XXCC	EiRabC8	EIN_168870	61	190	XXCC
RabD	EhRabD1	XP_652887	EHI_059670	751	XXCC	EiRabD	EIN_184580	61	744	XXCC
	EhRabD2	XP_655208	EHI_164900	265	XXCC					
RabF	EhRabF1	XP_651799	EHI_129740	203	CXXX	EiRabF1	EIN_239370	68	201	CXXX
	EhRabF2	XP_651513	EHI_182030	194	XXCC	EiRabF2	EIN_106040	61	192	XXCC
	EhRabF3	XP_655210	EHI_164880	191	XXCC	EiRabF3	EIN_112540	70	188	XXCC
	EhRabF4	XP_654217	EHI_122870	191	XXCC	EiRabF4	EIN_239300	65	192	XXCC
	EhRabF5	XP_656060	EHI_117960	197	XXXC	EiRabF5	EIN_228360	85	196	XXXC
RabH	EhRabH1	XP_657074	EHI_133100	209	XCXC	EiRabH	EIN_156660	78	217	XXCC
	EhRabH2[a]	XP_654758	EHI_128180	209	XCXC					
RabI	EhRabI1	XP_655925	EHI_177550	202	XCXC	EiRabI	EIN_014210	65	204	XXCC
	EhRabI2	XP_654235	EHI_053420	214	XCXC					
RabK	EhRabK1	XP_652298	EHI_024680	213	XXCC	EiRabK1	EIN_311490	81	210	XXCC
	EhRabK2	XP_649362	EHI_040450	210	XXCC	EiRabK2	EIN_243000	65	200	XXCC
	EhRabK3	XP_651827	EHI_082550	234	XXCC					
	EhRabK4	XP_648284	EHI_128110	243	XXCC	EiRabK4	EIN_059050	40	227	XXCC
	EhRabK5[a]	XP_655343	EHI_012380	240	XXCC	EiRabK5	EIN_028700	47	226	XXCC

RabL	EhRabL1	XP_651210	EHI_169090	207	XCCX	EiRabL1	EIN_081690	55	202	XXCC
	EhRabL2	XP_648952	EHI_069500	257	XCCX	EiRabL2	EIN_061000	52	210	XCCX
RabM	EhRabM1	XP_652833	EHI_005010	212	XXCC	EiRabM1	EIN_054310	73	213	XXCC
	EhRabM2	XP_652253	EHI_004380	204	XXCC					
	EhRabM3	XP_651723	EHI_068230	205	XXCC	EiRabM3	EIN_052610	79	174	XXCC
RabN	EhRabN1	XP_652702	EHI_048250	202	XCXX	EiRabN1	EIN_136950	71	201	CXXX
	EhRabN2	XP_649426	EHI_097650	199	XXXC	EiRabN2	EIN_054510	68	199	XXXC
RabP	EhRabP1	XP_651771	EHI_114210	204	CXXX	EiRabP	EIN_298880	59	205	CXXX
	EhRabP2	XP_656067	EHI_117890	204	CXXX					
RabX1	EhRabX1	XP_650791	EHI_017740	191	XXCC	EiRabX1A	EIN_299880	49	167	–
						EiRabX1B	EIN_111560	53	190	XXCC
RabX2	EhRabX2	XP_650041	EHI_001870	205	XXCC	EiRabX2A	EIN_134920	57	193	–
						EiRabX2B	EIN_099000	64	186	CXXX
RabX3	EhRabX3	XP_655050	EHI_014220	202	XXXC	EiRabX3[c]	EIN_135850	47	340	–
RabX4	EhRabX4	XP_651716	EHI_100090	195	XXCX	EiRabX4	EIN_240170	44	191	XXCX
RabX5	EhRabX5	XP_657472	EHI_148660	217	XXXC					
RabX6	EhRabX6	XP_652555	EHI_008350	201	CXXX	EiRabX6	EIN_123740	54	191	CXXX
RabX7	EhRabX7	XP_654103	EHI_118920	197	CXXX	EiRabX7	EIN_186210	47	204	CXXX
RabX8	EhRabX8	XP_649911	EHI_178040	210	CCXX					
RabX9	EhRabX9	XP_654197	EHI_140770	183	XXCC	EiRabX9	EIN_243270	45	190	XXCC
RabX10	EhRabX10	XP_656920	EHI_096440	189	CCXXX	EiRabX10	EIN_160760	45	193	CCXXX
RabX11	EhRabX11	XP_655922	EHI_177520	210	XXCC	EiRabX11A	EIN_014910	84	209	XXCC
						EiRabX11B	EIN_059070	77	209	XXCC
						EiRabX11C	EIN_092300	44	205	–
RabX12	EhRabX12	BAD82860	EHI_021210	199	XXCC	EiRabX12	EIN_252860	51	209	XXCC
RabX13	EhRabX13	XP_653656	EHI_065790	208	XXCC					
RabX14	EhRabX14	XP_657126	EHI_053150	354	XXCC	EiRabX14A	EIN_260390	42	228	XXCC
						EiRabX14B	EIN_147580	46	354	XXCC
RabX15	EhRabX15	XP_649287	EHI_177390	193	XXCC	EiRabX15	EIN_238750	65	192	XXCC
RabX16	EhRabX16	XP_655529	EHI_131170	204	XXCC	EiRabX16	EIN_051300	47	214	XXCC
RabX17	EhRabX17	XP_656536	EHI_042250	201	CXXX	EiRabX17A	EIN_072650	68	197	CXXX
						EiRabX17B	EIN_212470	57	197	CXXX
						EiRabX17C	EIN_107380	51	208	CCXXX
RabX18	EhRabX18A	XP_649285	EHI_145720	196	CXXX					
	EhRabX18B[a]	XP_001913559	EHI_177410	194	CXXX					
			EHI_008640							
RabX19	EhRabX19	XP_654968	EHI_183080	207	XXCC	EiRabX19	EIN_288570	46	226	XXCC
RabX20	EhRabX20	XP_652547	EHI_003020	190	XXCC					
RabX21	EhRabX21	XP_650747	EHI_021480	212	CXXXXX					
RabX22	EhRabX22A	XP_655103	EHI_157890	197	XXCC	EiRabX22A	EIN_134610	68	197	XXCC
	EhRabX22B[a]	XP_655064	EHI_014060	197	XXCC	EiRabX22B	EIN_075970	65	184	XXCC
						EiRabX22C	EIN_136400	62	197	XXCC
RabX23	EhRabX23	XP_650671	EHI_107140	187	XXCC	EiRabX23	EIN_241550	76	202	XXCC
RabX24	EhRabX24	XP_656866	EHI_038680	203	XXCC					
RabX25	EhRabX25	XP_653064	EHI_010660	192	XXCC	EiRabX25	EIN_243640	64	189	XXCC
RabX26	EhRabX26	XP_657341	EHI_151610	202	XXCC	EiRabX26	EIN_224230	50	198	XXCC
						EiRabX26B	EIN_060100	40	201	XCXC
RabX27	EhRabX27	XP_650814	EHI_158170	203	CXXX					
RabX28	EhRabX28	XP_647919	EHI_123220	186	CXXX					
RabX29	EhRabX29	XP_656310	EHI_184670	194	CXXX	EiRabX29	EIN_051680	64	198	CXXX
RabX30	EhRabX30	XP_651921	EHI_082230	183	CXXX	EiRabX30	EIN_148610	54	210	CXXX
			EHI_012030							
RabX31	EhRabX31	XP_648905	EHI_040310	194	XXCC	EiRabX31A	EIN_127810	70	189	XXCC
						EiRabX31B	EIN_262240	62	191	XXCC
						EiRabX31C	EIN_191990	42	170	XCXC
						EiRabX31D	EIN_197670	43	170	XCXC
RabX32	EhRabX32	XP_651095	EHI_079230	203	CXXXXX					
RabX33	EhRabX33A	XP_655812	EHI_083390	240	CCXXX					
	EhRabX33B[a]	XP_001914333	EHI_135940	248	CCXXX					

(continued on next page)

Table 1 (*continued*)

Rab subfamily	*Entamoeba histolytica*					*Entamoeba invadens*				
	EhRab isotype	Accession number	ID number	Protein length	C-terminal peptides	EiRab isotype	ID number	% Identity to Eh homologue	Protein length	C-terminal peptides
RabX34	EhRabX34	XP_650332	EHI_114640	200	CXXX	EiRabX34A	EIN_281740	68	204	CXXX
						EiRabX34B	EIN_202640	63	200	CXXX
RabX35	**EhRabX35**	**XP_649164**	**EHI_130670**	**195**	**XXCC**	**EiRabX35**	**EIN_156720**	**52**	**197**	**XXCC**
RabX36	EhRabX36	XP_657040	EHI_110300	203	–					
RabX37	**EhRabX37[a]**	**XP_652737**	**EHI_048720**	**184**	**XCXX**					
RabX38	EhRabX38[a]	XP_656081	EHI_118280	202	CCCXXX					
RabX39	**EhRabX39[a]**	**XP_649044**	**EHI_094110**	**180**	**XXCC**	**EiRabX39**	**EIN_238590**	**44**	**198**	**XXCC**
RabX40	EhRabX40[a]	XP_657549	EHI_027640	189	–	EiRabX40	EIN_105380	63	189	–
RabX41	**EhRabX41[a]**	**XP_001913412**	**EHI_051090**	**189**	**CXXX**	**EiRabX41**	**EIN_186350**	**52**	**191**	**CXXX**
RabX42	EhRabX42[a]	XP_651849	EHI_040330	180	CXXX					
III. Rab specific to E. histolytica										
RabX5	**EhRabX5**	**XP_657472**	**EHI_148660**	**217**	**XXXC**					
RabX8	EhRabX8	XP_649911	EHI_178040	210	CCXX					
RabX13	**EhRabX13**	**XP_653656**	**EHI_065790**	**208**	**XXCC**					
	EhRabX18A	XP_649285	EHI_145720	196	CXXX					
RabX18	EhRabX18B[a]	XP_001913559	EHI_177410	194	CXXX					
			EHI_008640							
RabX20	**EhRabX20**	**XP_652547**	**EHI_003020**	**190**	**XXCC**					
RabX21	EhRabX21	XP_650747	EHI_021480	212	CXXXXX					
RabX24	**EhRabX24**	**XP_656866**	**EHI_038680**	**203**	**XXCC**					
RabX27	EhRabX27	XP_650814	EHI_158170	203	CXXX					
RabX28	**EhRabX28**	**XP_647919**	**EHI_123220**	**186**	**CXXX**					
RabX32	EhRabX32	XP_651095	EHI_079230	203	CXXXXX					
RabX33	**EhRabX33A**	**XP_655812**	**EHI_083390**	**240**	**CCXXX**					
	EhRabX33B[a]	**XP_001914333**	**EHI_135940**	**248**	**CCXXX**					
RabX36	EhRabX36	XP_657040	EHI_110300	203	–					
RabX37	**EhRabX37[a]**	**XP_652737**	**EHI_048720**	**184**	**XCXX**					
RabX38	EhRabX38[a]	XP_656081	EHI_118280	202	CCCXXX					
RabX42	**EhRabX42[a]**	**XP_651849**	**EHI_040330**	**180**	**CXXX**					
IV. Rab specific to E. invadens										
RabZ1						**EiRabZ1**	**EIN_050800**		**204**	**XXCC**
RabZ2						EiRabZ2A	EIN_289320		200	CXXX
						EiRabZ2B	EIN_285540		198	CXXX
RabZ3						**EiRabZ3**	**EIN_192430**		**205**	**XXCC**
RabZ4						EiRabZ4A	EIN_297180		205	CXXX
						EiRabZ4B	EIN_234530		195	CXXX
RabZ5						**EiRabZ5**	**EIN_039070**		**203**	**XXCC**
RabZ6						EiRabZ6	EIN_051060		187	XXCC
RabZ7						**EiRabZ7**	**EIN_058330**		**207**	**XXCC**
RabZ8						EiRabZ8A	EIN_270650		191	CXXX
						EiRabZ8B	EIN_261500		150 (partial)	
RabZ9						**EiRabZ9**	**EIN_281720**		**203**	**XXCC**
RabZ10						EiRabZ10	EIN_105040		234	CCXXC
RabZ11						**EiRabZ11**	**EIN_256390**		**207**	**CXXX**
RabZ12						EiRabZ12	EIN_038850		207	CCXX
RabZ13						**EiRabZ13**	**EIN_016980**		**198**	**XXCC**
RabZ14						EiRabZ14	EIN_061010		147 (partial)	–
RabZ15						**EiRabZ15**	**EIN_050890**		**212**	**CXXX**
RabZ16						EiRabZ16	EIN_071820		195	CXXX
RabZ17						**EiRabZ17**	**EIN_200260**		**181**	**CXXX**
RabZ18						EiRabZ18	EIN_020600		204	XCCX
RabZ19						**EiRabZ19**	**EIN_017280**		**200**	**XXCC**
RabZ20						EiRabZ20	EIN_238400		184	CXXC

	EiRabZ21	EIN_089250	201	CXXX
RabZ21		EIN_026250		
		EIN_169660		
		EIN_169890		
RabZ22	EiRabZ22	EIN_165400	213	CXXXXXXX
RabZ23	**EiRabZ23**	**EIN_155360**	**200**	-
RabZ24	EiRabZ24	EIN_055510	230	CXXX
RabZ25	**EiRabZ25**	**EIN_111890**	**204**	XXCC
RabZ26	EiRabZ26	EIN_244150	184	CXXX

The annotations of *E. histolytica* Rabs are based on a previous publication (Saito-Nakano et al., 2005). The annotations of *E. invadens* Rabs were made on the basis of their percentage identity to the closest *E. histolytica* homologue and by phylogenetic inferences (Fig. 1).

[a] Newly found *E.histolytica* Rab genes in this study.

[b] 32% homology to EhRab21.

[c] EiRabX3 contains two GTPase domains.

2. Methods

2.1. Survey of Rab GTPases in the E. invadens and E. histolytica genome databases

Nucleotide and protein sequences of *S. cerevisiae* and *H. sapiens* Rabs were retrieved from GenBank, National Center of Biotechnology Information (NCBI). For the accession numbers of these proteins, see (Pereira-Leal and Seabra, 2001). We searched the *E. invadens* genome database (http://pathema.jcvi.org/cgi-bin/Entamoeba/PathemaHomePage.cgi) using all yeast and human Rab protein as queries by BLASTP. The *E. invadens* genome database was also searched by BLASTP using EiRab1A as a query. All potential small GTPase genes were further examined by BLASTP analysis against the human database at NCBI; *E. invadens* entries that showed the highest homology to Rab from *Entamoeba* or other organisms were considered to be *E. invadens* Rabs. The *E. histolytica* genome database (release 7.0) at Pathema Bioinformatics Resource Center (http://pathema.jcvi.org/Pathema/) was also searched and 11 previously unannotated *E. histolytica* Rab genes were identified. One hundred and twenty-one *E. invadens* and 11 newly found *E. histolytica* small GTPases were manually inspected to verify the presence of three GTP-binding consensus sequences (GDXXVGKT, DTAGQE, and GNKXD) and five additional conserved regions that are specific to the Rab family (IGVDF, KLQIW, RFRSIT, YYRGA, and LVYDIT) (Pereira-Leal and Seabra, 2000). One hundred and two *E. histolytica* and 121 *E. invadens* putative Rabs were designated according to the previous nomenclature (Saito-Nakano et al., 2005).

2.2. Phylogenetic analysis

Highly conserved domains stretching from the first to the third GTP-binding consensus regions of *E. histolytica*, *E. invadens*, *S. cerevisiae*, and *H. sapiens* Rab proteins were aligned using the CLUSTAL W program version 1.81 (Thompson et al., 1994) with default parameters. Alignments were manually inspected and corrected, and gaps were removed. Finally, 110 unambiguously aligned sites were selected for phylogenetic analysis by the neighbor-joining method (Saitou and Nei, 1987). Phylogenetic trees were drawn using TreeView software (http://taxonomy.zoology.gla.ac.uk/rod/rod.html).

3. Results and discussion

3.1. Annotation and conservation of E. invadens Rabs

3.1.1. Identification of new E. histolytica Rabs

We previously annotated 91 Rab genes in *E. histolytica* using the *E. histolytica* genome database available at TIGR (as of February 24, 2005; Saito-Nakano et al., 2005). A thorough search of the latest genome database at Pathema (version 7.0) identified 11 additional Rab genes; accordingly the current number of *E. histolytica* Rab genes increased to 102 (Table 1). The newly identified genes were annotated as RabH2, K5, X18B, X22B, X33B, and X37–42 (Table 1).

3.1.2. Assignment of E. invadens Rabs

We identified 121 putative Rab genes in the *E. invadens* genome database at Pathema. The number of *E. invadens* Rab genes was 20% higher than that of *E. histolytica*. *E. invadens* Rab entries were grouped based on their similarity to the corresponding *E. histolytica* homologues and also by phylogenetic inference (Table 1 and Fig. 1). Among the ubiquitous Rabs conserved in eukaryotes (Rab1~21), all isotypes of Rab1/8, 2, 5, 7, and 11 subfamilies that are present in *E. histolytica* are conserved in *E. invadens*, with the

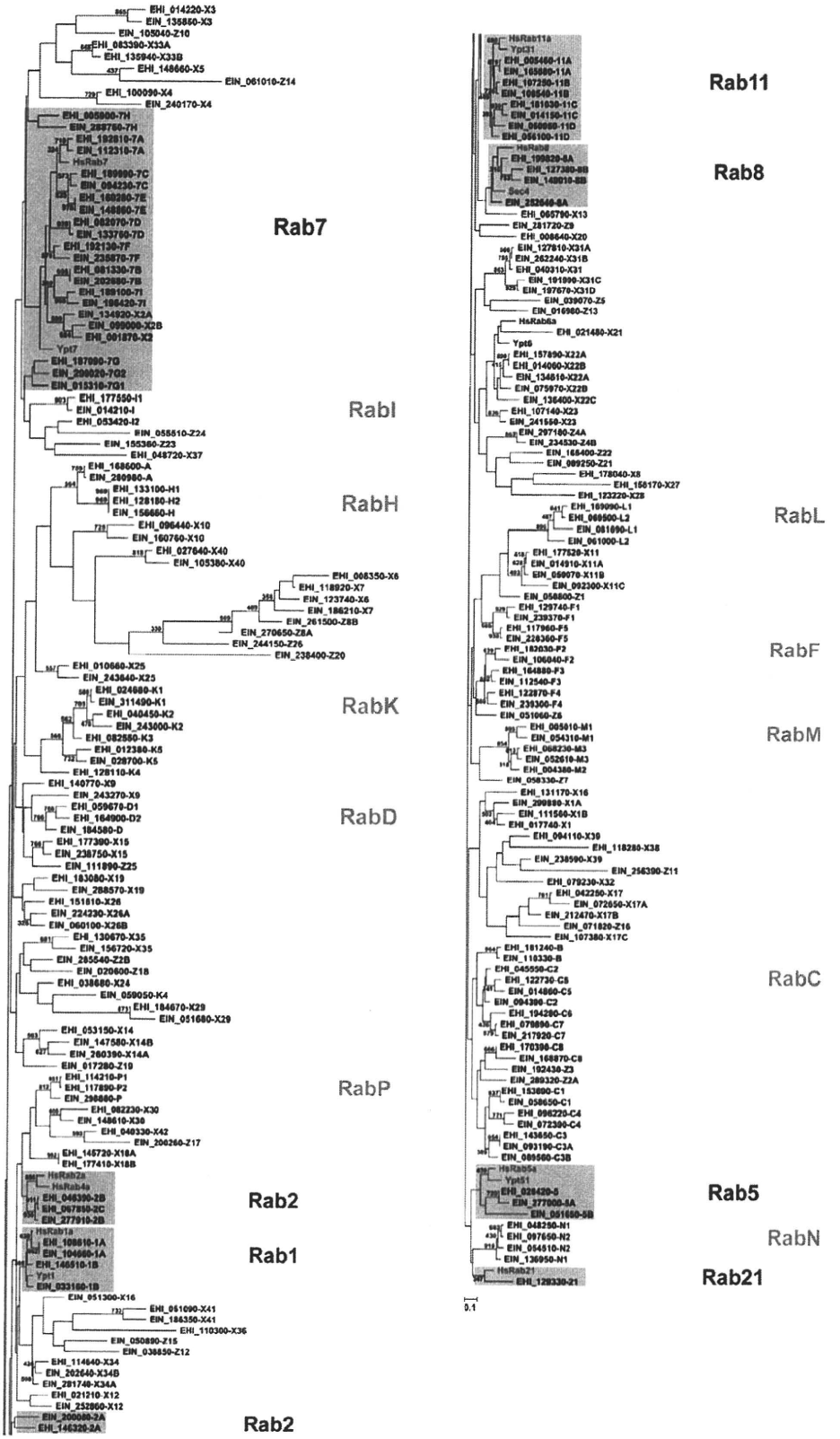

Fig. 1. Phylogenetic analysis of Rab proteins from *E. histolytica*, *E. invadens*, yeast and humans. Phylogenetic analysis of Rab genes from *E. histolytica*, *E. invadens*, yeast, and humans was performed using CLUSTAL W. Trees were drawn using TreeView. The numbers at the nodes represent bootstrap values for 1000 iterations shown in percentages. Yeast and human Rabs are indicated by Ypt and HsRab, respectively. Rabs from *E. histolytica* and *E. invadens* are indicated with their identification number (Table 1; starting with EHI or EIN for *E. histolytica* or *E. invadens* entries, respectively) followed by the subfamily name and number in its abbreviated form. Subfamilies that revealed significant homology (>40% identity) to yeast and human (e.g., Rab5) are shown in dark shaded boxes, while *Entamoeba*-specific subfamilies that contain multiple isotypes are shown in light shaded boxes. The scale bar indicates 0.1 substitutions at each amino acid.

exception of Rab2C. The relative proportion of ubiquitous Rabs conserved in eukaryotes (Rab1~21), *Entamoeba*-specific (i.e., conserved in the two *Entamoeba* species, but not present in other eukaryotes) Rabs (RabA~Z), and species-specific Rabs are similar between *E. histolytica* and *E. invadens* (Fig. 2).

3.1.3. Rabs conserved between E. histolytica and E. invadens

Some Rab subfamilies or isotypes consist of different numbers of isotypes or subisotypes in *E. histolytica* and *E. invadens* (Table 2). Eighty-five percent of Rabs that form subfamilies (e.g., RabC) are conserved (Table 1), suggesting the shared house-keeping roles of these Rab subfamilies in *Entamoeba*. The only exceptions are the RabX18 and RabX33 subfamilies that consist of two isotypes in *E. histolytica*, but are not conserved in *E. invadens*. Conversely, 38% of the solitary (i.e., not forming a subfamily) Rabs are not conserved in *E. invadens*.

3.1.4. Rabs specific to E. histolytica or E. invadens

Among Rab proteins conserved in eukaryotes (Rab1~21), *E. invadens* has additional isotypes of Rab5 and Rab7G, EiRab5B and EiRab7G2, respectively. *E. histolytica* has one each of EhRab5 and EhRab21 that are categorized into the Rab5/Rab21 group (Pereira-Leal and Seabra, 2001). While two EiRab5 isotypes show a 50–83% identity to EhRab5, they show only a 32–33% identity to EhRab21, and were thus annotated as a Rab5 isotype. Phylogenetic analysis (Fig. 1) also supported this annotation.

The number of isotypes and subisotypes in 12 subfamilies and isotypes (Rab5B, 7G2, C3, X1B, X2B, X11B–C, X14B, X17B–C, X22C, X26B, X31B–D, and X34B) is higher in *E. invadens* than in *E. histolytica* (Table 2). In addition, 29 *E. invadens* Rabs (EiRabZ1–26) that show low (<40%) similarity to *E. histolytica* Rabs were discovered and considered to have independently evolved in *E. invadens*. Conversely, homologues corresponding to 26 *E. histolytica* Rabs were not identified in the current *E. invadens* database; however, the lack of these Rabs in *E. invadens* must be confirmed due to the lower coverage of the *E. invadens* genome.

3.2. Review of the demonstrated functions of Rabs in Entamoeba

Although several previous proteomic and transcriptomic studies (see below) suggested that a few dozens of Rab genes/proteins are involved in important biological processes, such as stress response, pathogenesis, and stage conversion, these Rab genes were not discussed. This is partly due to the lack of proper annotation of *Entamoeba* Rab genes at the time of publication. In this section, we summarize the current understanding of the reported functions of Rabs, and also review the previous transcriptomic and proteomic studies that indicate the roles of Rab genes in stress response, pathogenesis, and stage conversion.

Table 2
Rab subfamilies and isotypes that vary in number between *E. histolytica* and *E. invadens*. Seventeen Rab families that have different numbers of isotypes and two isotypes (EhRab7G and EhRabC3) that are encoded by two independent genes are shown.

Rab subfamily/isotype	Number of Rab isotypes	
	E. histolytica	*E. invadens*
Rab2	3	2
Rab5	1	2
Rab7G	1	2
RabC3	1	2
RabD	2	1
RabH	2	1
RabI	2	1
RabK	5	4
RabM	3	2
RabP	2	1
RabX1	1	2
RabX2	1	2
RabX11	1	3
RabX14	1	2
RabX17	1	3
RabX22		3
RabX26	1	2
RabX31	1	4
RabX34	1	2

3.2.1. Demonstrated functions of E. histolytica Rabs

Among all annotated Rabs, there are only a dozen for which their localization, function, or both have been demonstrated. Among the multiple EhRab7 isotypes, EhRab7B is involved in lysosome biogenesis (Fig. 3; Saito-Nakano et al., 2007), while EhRab7A is involved in the targeting of hydrolases to lysosomes (Nakada-Tsukui et al., 2005; Saito-Nakano et al., 2007). EhRab7A, together with EhRab5, also coordinately regulates the formation and matu-

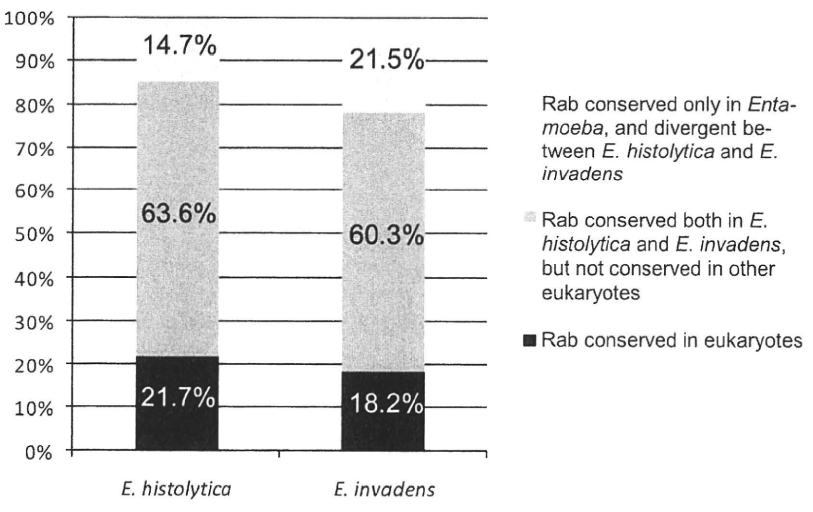

Fig. 2. Percentages of conserved and genus- or species-specific Rab genes in *E. histolytica* and *E. invadens*. Percentage of Rab genes conserved in eukaryotes (Rab1~21, black bars), Rab genes conserved in *E. histolytica* and *E. invadens*, but not conserved in other eukaryotes (RabA~Z, dark shaded bars), and Rab genes conserved only in *Entamoeba* and divergent between *E. histolytica* and *E. invadens* (light shaded bars).

ration of the prephagosomal vacuole (PPV), a unique organelle in *E. histolytica* that is formed during phagocytosis, and is likely to be involved in the processing, activation, or storage of hydrolases that are transported to the phagosome (Saito-Nakano et al., 2004). *E. histolytica*-specific EhRabA was initially suggested to be involved in motility and polarization (Welter et al., 2005), and has been recently shown to be involved in the transport of the Gal/GalNAc-specific lectin (Welter and Temesvari, 2009). EhRab11A was reported to be recruited to the cell surface by iron or serum starvation, and was suggested to be involved in encystation (McGugan and Temesvari, 2003). In contrast, EhRab11B is involved in cysteine protease secretion, and its overexpression enhanced the secretion of cysteine protease (Mitra et al., 2007).

The proteomic analysis of phagosomes isolated from *E. histolytica* trophozoites revealed a panel of phagosome-associated Rabs (Fig. 3; Marion et al., 2005; Okada et al., 2005, 2006). Among the phagosome-associated Rabs, RabD2, P2, and X37 are not conserved in *E. invadens* (Table 1). Interestingly, EhRabD2 and EhRabX37 were expressed only in trophozoites, but not in cysts; their expression was also downregulated during oxidative stress (Table 3, see below). The role of these Rabs appears to be specific to *E. histolytica*, and may be associated with virulence. It needs to be confirmed by proteomic analysis of isolated *E. invadens* phagosomes whether Rab proteins and other phagosome proteins are shared by both species.

3.2.2. Stress- or infection-induced regulation of Rab gene expression

Previous transcriptomic studies indicated that several Rab genes are transcriptionally regulated during stress, stage conversion, and animal infection (Table 3). Incubation of trophozoites at 42 °C for 1 h caused the upregulation of the EhRab7A gene by 2-fold (MacFarlane et al., 2005). It was also shown that the levels

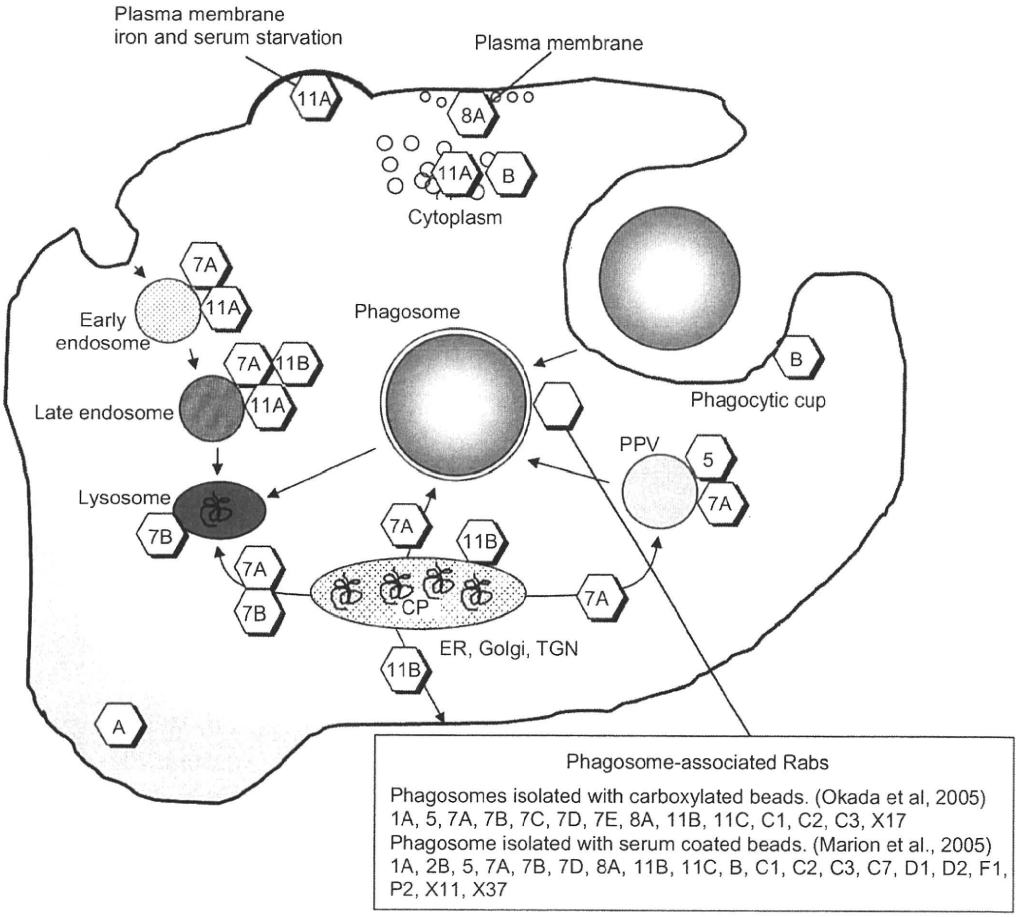

Fig. 3. Demonstrated and presumed localization and function of *E. histolytica* Rabs. Summarized scheme of the localization and function of selected *E. histolytica* Rab proteins is shown based on previous publications. (1) Endosomes: EhRab7A, EhRab11A, and EhRab11B were demonstrated to be localized to endosomes by immunofluorescence assay (EhRab7A and EhRab11B), or immunoblot analysis using iron-dextran-containing endosomes isolated using magnetic separation (EhRab7A and EhRab11A) (Temesvari et al., 1999; Saito-Nakano et al., 2004; Nakada-Tsukui et al., 2005; Mitra et al., 2007). EhRab11A was not demonstrated to be located on endosomes by immunofluorescence, but was suggested to be translocated to the cell surface upon iron and serum starvation or encystation (McGugan and Temesvari, 2003). (2) Phagosomes: EhRabB was localized to the phagocytic cup (Rodriguez et al., 2000). Phagosome-associated Rab proteins, demonstrated by proteomic analysis of isolated phagosomes using carboxylated beads (Okada et al., 2005) or serum-coated beads (Marion et al., 2005), are found in the islet. All Rab proteins detected at various time points of phagocytosis in different strains are listed. (3) Prephagosomal vacuoles (PPV): PPV were reported to be a reservoir of cysteine proteases and other digestive enzymes transported to the phagosome, and EhRab5 and EhRab7A were localized to PPV (Saito-Nakano et al., 2004). (4) Lysosomes: EhRab7A is involved in the transport of cysteine proteases to phagosomes and lysosomes, and a partial association of EhRab7A with lysosomes was observed (Nakada-Tsukui et al., 2005; Saito-Nakano et al., 2007). EhRab11B was suggested to be involved in the transport of cysteine proteases (Mitra et al., 2007), although its exact localization remains unknown. EhRab7B was present in lysosomes and involved in lysosome biogenesis, together with EhRab7A (Saito-Nakano et al., 2007). (5) Secretory vesicles or post-Golgi compartments: EhRab8 showed peripheral dotted localization underneath the plasma membrane, and was suggested to be involved in secretion (Juarez et al., 2001). (6) Unknown compartments in the cytoplasm: EhRabB revealed a punctate dotted localization throughout the cytoplasm, but its exact localization remains to be determined (Rodriguez et al., 2000). EhRabA was localized to the leading edge of the cell and was presumed to regulate cell motility and polarization (Welter and Temesvari, 2004; Welter et al., 2005). Furthermore, the overexpression of dominant negative EhRabA caused an alteration of ER morphology and the localization of the Gal/GalNAc-specific lectin (Welter and Temesvari, 2009).

Table 3
Rab genes that are differentially expressed.

Rab gene	Fold change	Up/down	Condition/stage/strain	Method[a]	Reference[b]
Ehrab5	3.62	Down	Cyst (vs. trophozoite)	D	a
	3.2	Down	*E. dispar* (vs. *E. histolytica*)	D	b
Ehrab7A	2	Up	Heat shock[c]	D	c
Ehrab7D	25.37	Up	Avirulent HM-1 (vs. virulent HM-1)	D	d
	3.55	Down	Cyst (vs. trophozoite)	D	a
Ehrab7E	62	Up	Avirulent HM-1 (vs. virulent HM-1)	D	d
Ehrab7F	4.8	Down	Oxidative stress[e], HM-1	D	e
	4.4	Down	NO stress[f]	D	
Ehrab7G	14.5	Up	Avirulent HM-1 (vs. virulent HM-1)	D	d
Ehrab11A	4.23	Down	Cyst (vs. trophozoite)	D	a
Ehrab11B	4.55	Down	Cyst (vs. trophozoite)	D	a
Ehrab11D	8.43	Down	Cyst (vs. trophozoite)	D	a
EhrabB	5	Up	Heat shock[d]	P	f
	3.32	Down	Cyst (vs. trophozoite)	D	a
EhrabC1	2.2	Down	Cyst (vs. trophozoite)	D	a
EhrabC2	2.2	Down	NO stress[f]	D	e
EhrabC5	3.66	Down	Cyst (vs. trophozoite)	D	a
EhrabC6	6.15	Down	Cyst (vs. trophozoite)	D	a
EhrabD2	5.52	Down	Cyst (vs. trophozoite)	D	a
	2.8	Down	Oxidative stress[e], HM-1	D	e
EhrabH1	3.41	Down	Cyst (vs. trophozoite)	D	a
EhrabI1	3.56	Up	Oxidative stress[e], HM-1	D	e
	3.5	Up	NO stress[f]	D	
EhrabK2	7.14	Down	Cyst (vs. trophozoite)	D	a
EhrabL1	2.7	Down	NO stress[f]	D	e
EhrabM1	6.7	Up	Cyst (vs. trophozoite)	D	a
	2	Up	Oxidative stress[e], HM-1	D	e
EhrabM2	3.65	Down	Cyst (vs. trophozoite)	D	a
EhrabNI	4.1	Up	Cyst (vs. trophozoite)	D	a
EhrabX6	4.76	Down	*E. dispar* (vs. *E. histolytica*)	D	b
EhrabX13	2	Down	*E. dispar* (vs. *E. histolytica*)	D	b
EhrabX14	2.95	Up	Day 1 of intestinal challenge	D	g
	2.86	Up	Day 29 of intestinal challenge	D	
EhrabX15	3	Up	NO stress[f]	D	e
EhrabX19	5.1	Down	NO stress[f]	D	e
EhrabX31	2	Up	Oxidative stress[e], Rhaman	D	e
EhrabX32	2.7	Up	NO stress[f]	D	e
EhrabX35	2.3	Up	Oxidative stress[e], Rhaman	D	e
	2	Up	NO stress[f]	D	
EhrabX37	3.84	Down	Cyst (vs. trophozoite)	D	a
EhrabX42	2.43	Down	NO stress[f]	D	e

[a]D, DNA microarray; P, real-time PCR.
[b](a) Ehrenkaufer et al. (2007), (b) MacFarlane and Singh (2006), (c) MacFarlane et al. (2005), (d) Biller et al. (2010), (e) Vicente et al. (2009), (f) Romero-Diaz et al. (2007), (g) Gilchrist et al. (2006).
[c]42 °C, 1 h.
[d]42 °C, 5 h.
[e]1 mM H_2O_2, 1 h.
[f]HM-1, 200 μM dipropylenetriamine (DPTA)-NONNate, 1 h.

of the EhRabB transcript increased by 5-fold after incubation at 42 °C for 5 h (Romero-Diaz et al., 2007). It was suggested that the putative heat shock elements (HSE) upstream of the EhRabB gene are involved in the regulation of EhRabB (Romero-Diaz et al., 2007). It was also shown that incubation of trophozoites from the HM-1 and Rhaman strains with hydrogen peroxide or the nitric oxide donor dipropylenetriamine-NONOate (DPTA), caused a 4-fold upregulation of EhRabI1, and a 4.4–4.8-fold downregulation of EhRab7F (Vicente et al., 2009). Since these Rabs appeared to be regulated in a similar way by hydrogen peroxide and nitric oxide, common regulator(s) and pathway(s) may be involved in the responses against these stresses. It should be noted that some Rab genes differentially respond to oxidative and nitric oxide stress. For example, EhRabM1 and EhRabX31 were upregulated only by hydrogen peroxide, while EhRabX15, X32, and X35 were upregulated only by DPTA (Vicente et al., 2009). Similarly, EhRabD2 was downregulated by oxidative stress, whereas EhRabC2, L1, and X19 were downregulated by nitric oxide (Vicente et al., 2009). Although the role of these Rabs remains unknown, these findings indicate a possible link between oxidative/nitrosative stress response and membrane trafficking. In addition, it was shown that during mouse intestinal infection, EhRabX14 expression was upregulated on days 1 and 29 post-infection (Gilchrist et al., 2006). These change in expression may also be a consequence of the stress response because amoebae are exposed to reactive oxygen and nitrogen species during host invasion.

3.2.3. Differences in Rab gene expression between E. histolytica and E. dispar, and between virulent and avirulent E. histolytica strains

A comparison of the transcriptome of the non-pathogenic sibling *E. dispar* and *E. histolytica* also revealed that Rab5, X6, and X13 were downregulated in *E. dispar* (MacFarlane and Singh, 2006). Since Rab5 plays a role in the formation of the PPV in *E. histolytica* (Saito-Nakano et al., 2004), the repression of Rab5 expression in *E. dispar* may indicate the suppressed activity of phagocytosis and endocytosis in *E. dispar* (Mitra et al., 2005). Recently, transcriptomic analysis of two HM-1 strains with different abilities to form amoebic liver abscess was reported (Biller et al., 2010). The expression of three Rab7 subfamilies, EhRab7D, 7E, and 7G, was augmented in the avirulent HM-1 strain, obtained